AD-A057 344 HOCHSCHULE DER BUNDESWEHR MUNICH (GERMANY F R) DEPT --ETC F/G 17/2.1
MOBA - RECEIVING SYSTEM WITH HIGH AVAILABILITY.(U)
MAY 78 G FLACHENECKER

UNCLASSIFIED DA-ERO-77-G-049

NL

| OF |
AD
A057 344

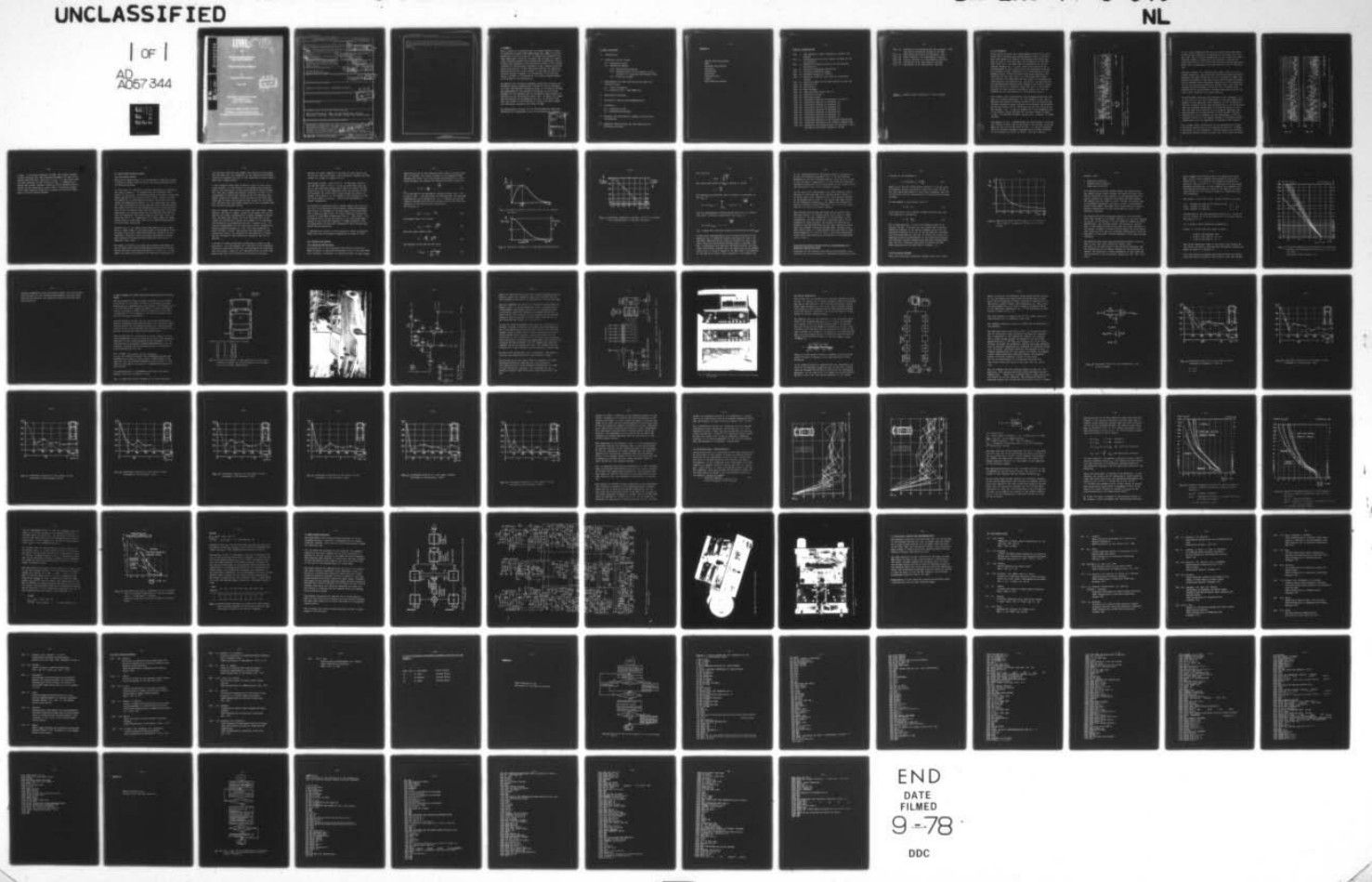

END
DATE
FILMED
9-78
DDC

LEVEL II

AD

MOBA-Receiving System with High Availability

Final Technical Report

by

Gerhard Flachenecker

May 1978

EUROPEAN RESEARCH OFFICE
United States Army
London NW 1, England

GRANT NUMBER DA-ERO-77-G-049

Department of Electrical Engineering
University of the German Armed Forces Munich

UNCLASSIFIED

SECURITY CLASSIFICATION OF THIS PAGE (When Data Entered)

REPORT DOCUMENTATION PAGE	READ INSTRUCTIONS BEFORE COMPLETING FORM
1. REPORT NUMBER	2. GOVT ACCESSION NO. / 3. RECIPIENT'S CATALOG NUMBER
4. TITLE (and Subtitle) MOBA - Receiving System with High Availability.	5. TYPE OF REPORT & PERIOD COVERED Final Technical Report. 1 Apr 77 - 31 Mar 78.
	6. PERFORMING ORG. REPORT NUMBER
7. AUTHOR(s) G. Flachenecker (Gerhard)	8. CONTRACT OR GRANT NUMBER(s) DA-ERO DAERO-77-G-049
9. PERFORMING ORGANIZATION NAME AND ADDRESS Department of Electrical Engineering University of the German Armed Forces Munich, Germany	10. PROGRAM ELEMENT, PROJECT, TASK AREA & WORK UNIT NUMBERS 6.11.02A/1T161102BH57-03-00 -656
11. CONTROLLING OFFICE NAME AND ADDRESS US Army R&S Gp (Eur) Box 65, FPO New York 09510	12. REPORT DATE May 78 / 13. NUMBER OF PAGES 87
14. MONITORING AGENCY NAME & ADDRESS (if different from Controlling Office)	15. SECURITY CLASS. (of this report) Unclassified / 15a. DECLASSIFICATION/DOWNGRADING SCHEDULE

16. DISTRIBUTION STATEMENT (of this Report)

Approved for public release; Distribution unlimited

DDC RECEIVED AUG 11 1978 F

17. DISTRIBUTION STATEMENT (of the abstract entered in Block 20, if different from Report)

18. SUPPLEMENTARY NOTES

19. KEY WORDS (Continue on reverse side if necessary and identify by block number)

Mobile receiving system; MOBA; Rayleigh distribution; Diversity; Correlation; Covariance; Diversity gain; Fading; Fade reduction factor.

20. ABSTRACT (Continue on reverse side if necessary and identify by block number)

To investigate fading effects of mobile receiving systems under MOBA-conditions, 6 antennas have been mounted in various spacings on a car and the covariance function of 9 different antenna combinations has been measured in the frequency range 30 to 300 MHz while driving the car. While in nearly all cases the presence of the conducting surface of the car increases correlation over the theoretically expected values, the correlation

78 08 08 145

DD FORM 1 JAN 73 1473 EDITION OF 1 NOV 65 IS OBSOLETE

S/N 393433

UNCLASSIFIED

SECURITY CLASSIFICATION OF THIS PAGE (When Data Entered)

factors are small enough for sufficient diversity gain above 30 Miz. An experimental receiver for the FM-broadcasting range has been developed for experimental use at the U.S. Army Electronics Research and Development Command.

1. Summary

This research is concerned with the fading effects of mobile receiving systems under MOBA-conditions (MOBA = military operations in built-up areas). To reduce the probability of deep fades space diversity antennas can be used if a sufficient distance between the antennas can be achieved. The diversity gain depends on the correlation factor of the output voltages of the different antennas in use. Theoretically the space distribution of the covariance function for Rayleigh distributed fields is well known. In the case of mobile receiving systems, however, the correlation of the antenna output voltages is influenced by the complex shaped conducting surface of the bearing car.

We measured the frequency dependent covariance function of 9 different antenna combinations mounted in various spacings on a car. The measured frequency range is 30 through 300 MHz. The dependence of the measured covariances on the linear distance of the antennas and the frequency shows obvious similarity to the theoretical values. But, in nearly all cases the correlation is increased by the car. In spite of this fact the values of the correlation factor are small enough for sufficient diversity gain above 30 MHz.

An experimental receiver for the FM-broadcasting range was developed for experimental use at the Electronics Command.

2. List of content

Keywords:

Mobile receiving system
MOBA
Rayleigh distribution
Diversity
Correlation
Covariance
Diversity gain
Fading
Fade reduction factor

List of Illustrations

3. Introduction

Within built-up areas the electromagnetic wave field generated from a transmitting system spaced inside or outside this area shows very complex fieldstrength distributions. This is true in the case where the wavelength of the radiated field is in the same order of dimensions of the obstacles (houses etc.) or less. Under this condition the fieldstrength at each place within the disturbed field can be regarded as being produced by the interference of many separate waves. These different waves are produced by reflections at the house walls, by scattering and diffraction effects. The magnitude and the phases of all waves are stochastically distributed and, therefore, the magnitude of the fieldstrength statistically changes from place to place. At some places the different waves add up to a high fieldstrength at other places a minimum or even a zero can be produced by the interference of the different waves.

This complex field distribution can be demonstrated with the help of a simple experiment. If, for example, a car with a FM-receiving system is moving through a city the rapidly and strongly changing output voltage of the antenna can be measured and the zeros can be recognized audibly with the help of the speaker. Fig. 1 gives an example of a time dependent plot of an antenna output voltage. The car had a speed of about 10 mph, the received FM-radio station had a frequency of about 100 MHz.

The example of Fig. 1 demonstrates the differences in the output voltage of more than 20 dB within a few seconds. From the speed of the car and the plot of Fig. 1 it can be evaluated that the distance between a maximum and an adjacent minimum in the average has values of about 1 through 4 meters.

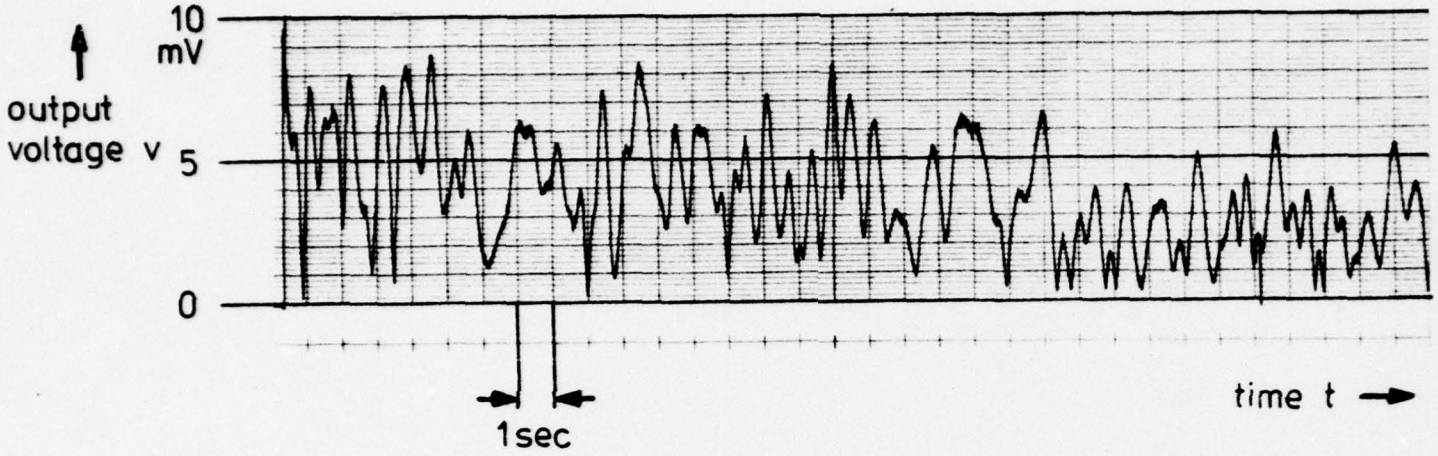

Fig. 1: Output voltage of an antenna mounted on a car, which is moving through a built-up area.
f ≈ 100 MHz; speed of the car V ≈ 10 mph

In the case of MOBA the car with the receiving system often is moving very slowly or is standing at one place for a longer time. With a certain probability at this place the field strength component which has to be received is below the noise level due to the interfering effects as mentioned above. Under this circumstances the communication link is interrupted.

Similar problems, for instance short wave reception or microwave scattering links have been solved with space diversity systems. The same technology should be possible in MOBA communication systems if the spatially field distribution essentially changes within distances comparable to the dimensions of the car bearing the receiving system. Then, more than one antenna could be mounted on the car with a reduced joint probability of having output voltages simultaneous below the noise level compared to a single antenna.

The attainable diversity gain depends on the frequency, i.e. on the ratio of the car's dimensions to the free space wavelength. A very important fact, however, is the influence of the car's surface on the wave distribution. It is not obvious that two antennas spaced apart a certain distance on a car show the same decorrelation as two antennas separated the same distance on a plane ground. On this account the main subjective of this research ist the measurement of the covariance function of the output voltage of different antenna combinations on a car dependent on frequency and location.

As a simple basic verification of the possibility of space diversity systems even on the surface of cars Fig. 2 shows the result of an experiment. A car now bearing two antennas was moved through a built-up area. The car's speed was about

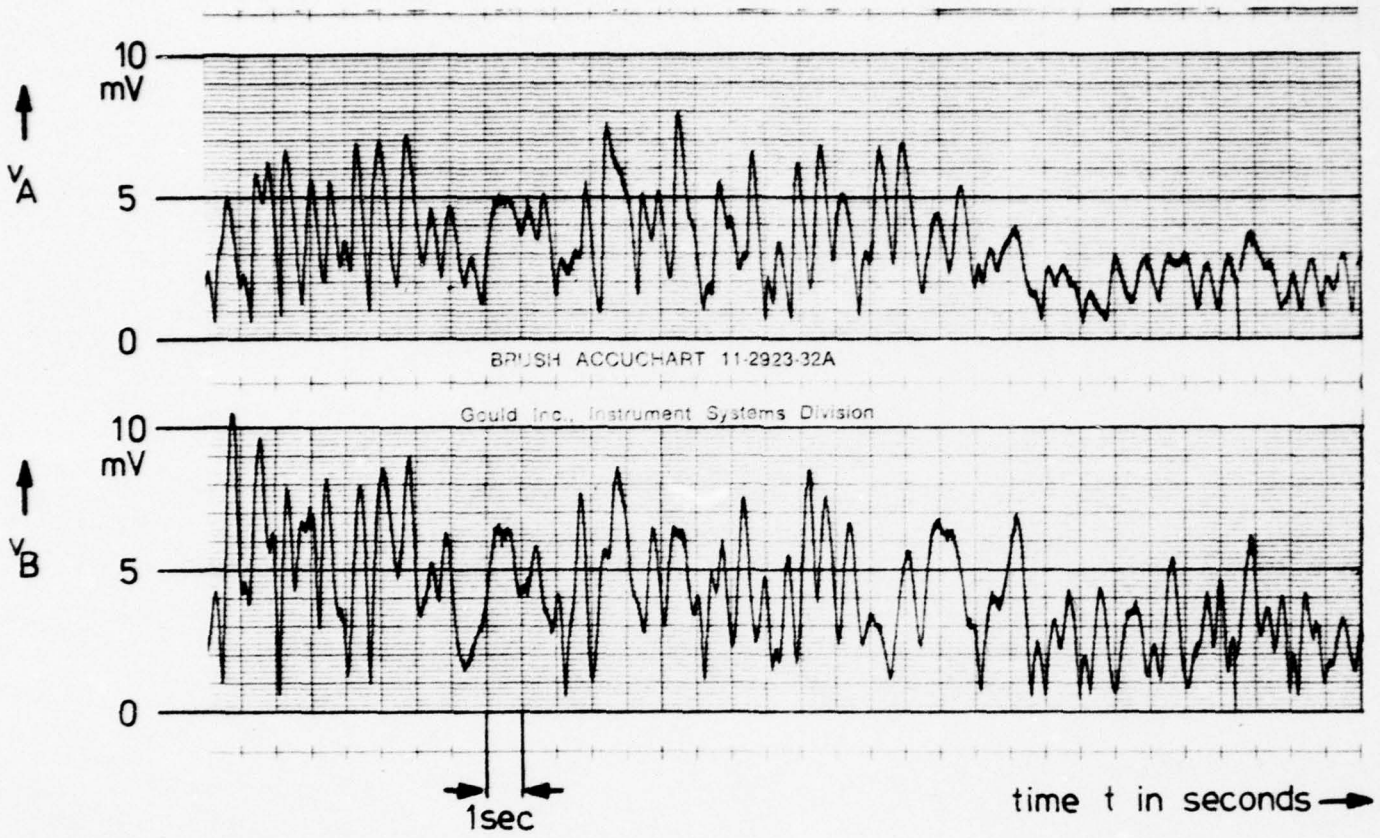

Fig. 2: Output voltages of two antennas mounted at different places of a car
Car speed v ≈ 10 mph. Received frequency f = 100 MHz

10 mph, the received frequency 100 MHz. The output voltages of both antennas have been measured dependent on time and recorded simultaneously. Each plot of Fig. 2 in principle shows the same behaviour as the antenna of Fig. 1. Comparing the minima and maxima, however, temporary shifts between both antennas can be recognized in most cases. A diversity system using these antennas would show a higher availability compared to a single antenna system.

4. Literature review; theory

4.1 Literature review

Many recent papers dealt with the problem of scattered fields in built-up areas as well as with the theory and application of diversity systems.

In 1952 Young /1/ started to evaluate UHF-field distributions for mobile reception in metropolitan and suburban areas. Ossana /2/ developed a reflecting model. It is able to describe power spectra of the received fading field. Several scattering models of the spatially distributed field have been evaluated and compared by Gilbert /3/. He showed that very similar field distributions can be obtained with different models. His models differed in the assumptions of the angle distribution of the N incoming waves and the distribution of the wave amplitudes. All authors find that the Rayleigh distribution fits the amplitude distribution best in the case where the receiving field is a composition of a large number of waves nearly equal in amplitude. This is the MOBA situation with no direct wave receiption.

Trifonov et.al. /4/ found a Rice distribution in all cases where a large number of reflected waves is adjoined by a significant direct wave, which describes the situation in the suburbans. Outside of built-up areas they found a non-zero mean Gaussian distribution describing the reception of a dominant direct wave.

The model of Gilbert with equal and constant amplitudes of all incoming waves and rectangularely distributed arriving angles has been evaluated extensively by Clarke /5/. In this paper the spatial distribution and covariance functions of

the Rayleigh field are calculated. The results of this paper are used here for the comparison of the measured correlation factors of antennas on a car to the theoretical values attainable over a plane ground.

A lot of papers deals with diversity reception with correlated signals. In 1955 Staras /6/ calculated the diversity gain of the receiption of correlated Rayleigh fading signals. The joint pdf (probability density function) of Rice /7/ is interpreted for equal mean values of the two Rayleigh variables. Vigants /8/ expands the evaluation of the joint Rayleigh pdf to cases with different mean values of the variables. He shows that deep fades essentially can be reduced even with highly correlated signals.

Gans /9/ expands the results of Clarke and calculates power spectra, duration of fades, random FM processes, and the diversity gain under consideration of space dependent correlation. He shows that nearly the full diversity gain is obtained for correlation factors up to about 0.7. A polarization diversity is proposed by Lee /10/. Parsons et.al. /11/ describe measurements on the correlation factor between differently spaced antennas on a car. The used frequency of about 100 MHz is fixed. The results are comparable to the theoretical values, for example the calculations of Clarke. But the increase of the correlation caused by the car is obvious.

A review of existing diversity techniques is given by Parsons et.al. /12/ and Brennan /27/. The gain of the selection diversity, equal-gain diversity, and maximum ratio diversity over the single reception of a Rayleigh field is given. The papers show that the differences of different diversity

systems are small compared to the gain of each system over the single receiving system. Other diversity systems are described in a number of papers /13-17/.

Some papers concern the reception of Rayleigh fields in the 900 MHz region /18-23/. It can be recognized that the car in the microwave region nearly does not effect the Rayleigh field. The field components along the surface of the car approach the field over a plane ground the better the higher the frequency is. The reason is the curvature of the car being nearly neglegable against the wavelength at higher frequencies.

At microwave frequencies and at higher speeds the motion of the car in the Rayleigh field produces random-FM processes. This effect is regarded in the most papers mentioned above and in special papers /24/. The main frequency spectra are limited to side band frequencies below $2 \cdot v/\lambda_o$, where v is the speed of the moving car and λ_o is the free space wavelength at the received frequency. In MOBA situations with low speed and at low military frequencies below 300 MHz this effect can be neglected.

A comprehensive review on the problems of mobile receiption under the view of microwave frequencies is given in /25/.

4.2 Theoretical Basics

4.21 Rayleigh Distribution

As pointed out in the literature the receiving field in a MOBA situation is Rayleigh distributed. This is the case when only reflected, scattered, or diffracted waves of about equal

magnitude arrive at the receivers site, while no direct wave can be received. The output voltage V of an antenna moved through this field can be described approximately as a Rayleigh variable the probability density function of which is

$$p\ (V) = \frac{2V}{\overline{V^2}} \cdot e^{-\frac{V^2}{\overline{V^2}}} . \qquad (1)$$

$\overline{V^2}$ is the RMS of the stochastic varying voltage. Fig. 3 is a Plot of equ. 1 and describes the Rayleigh pdf. The Rayleigh distribution is one dimensional, i.e. it shows only one parameter. The RMS value and the variance as well as other parameters of the function are proportional.
The variance is

$$\sigma^2 = 0.21 \cdot \overline{V^2} , \qquad (2)$$

the median value (50 % value)

$$V_m = 0.833 \cdot \sqrt{\overline{V^2}} \qquad (3)$$

and the linear medium value

$$\overline{V} = \frac{\sqrt{\pi}}{2} \sqrt{\overline{V^2}} . \qquad (4)$$

The maximum of the pdf has the value

$$p(V_{max}) = \frac{1}{\sqrt{e \cdot \frac{\overline{V^2}}{2}}} \qquad (5)$$

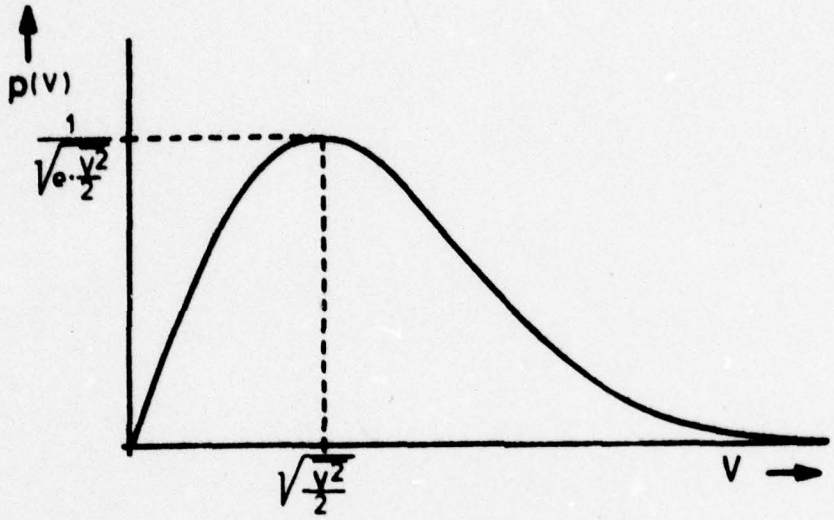

Fig. 3: Probability density function (pdf) of the Rayleigh variable V.

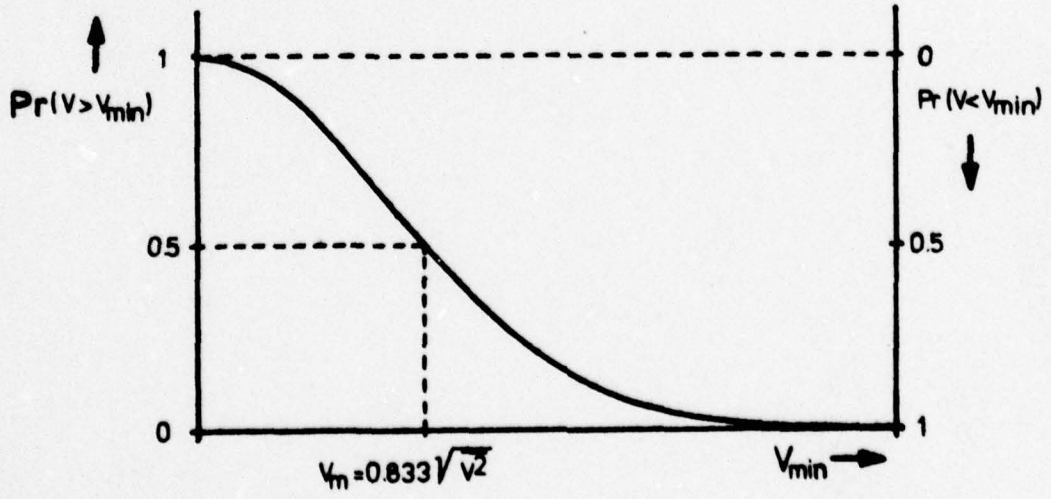

Fig. 4: Cumulative probability of the Rayleigh distribution

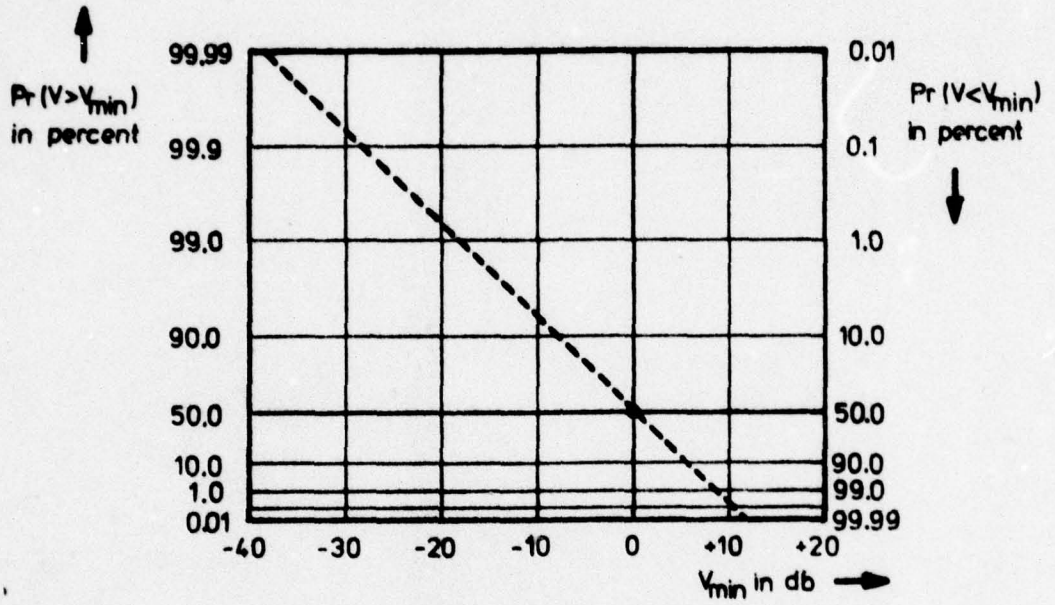

Fig. 5: Logarithmic Rayleigh coordinate system for straight-line representation of Rayleigh variables

at a value of

$$V_{max} = \sqrt{\frac{V^2}{2}} \quad . \tag{6}$$

The often used values of $V_{RMS}^2/2$ usually is called

$$b = \frac{V^2}{2} \quad . \tag{7}$$

The cumulative probability that V exceeds a prescribed level V_{min} is

$$Pr\ (V > V_{min}) = \int_{V_{min}}^{\infty} p(V)\, dV = e^{-\frac{V_{min}^2}{V^2}} \tag{8}$$

and the complementary function which describes the probability that V is below a prescribed level V_{min} is

$$Pr\ (V < V_{min}) = 1 - e^{-\frac{V_{min}^2}{V^2}} \tag{9}$$

Fig. 4 shows the cumulative Rayleigh distribution $Pr(V > V_{min})$.

A more plain representation which is better suited for the Rayleigh test of measured voltage distributions uses a logarithmic abscissa and an ordinate distorted in such a way that a Rayleigh distributed variable shows a straight line. Fig. 5 represents this Rayleigh coordinate system. All Rayleigh distributed voltages show the same slope as the dashed line in Fig. 5 without regard to the RMS value. A difference in the RMS only causes a shift parallel to the dashed line.

In the representations of measuring results in chapter 5.2 we use the coordinate system of Fig. 5. As the zero-dB standard we use the 50-percent(median) value of the voltage or the S/N ratio, respectivelv. If more than one different variable signals have to be represented in one figure we use the 50-percent value of the strongest signal.

In the case of our measurements the ideal Rayleigh distributions is fulfilled only in a limited range of about 15 to 20 dB. This range represents as a line section parallel to the dashed line in Fig. 5. For higher and lower values of the threshold voltage V_{min} the cumulative probability function deviates from the straight line. This is an accordance to the results of other authors.

The Rayleigh distribution describes the so-called "fast Rayleigh fading". In limited areas in the order of about 1/10 mile x 1/10 mile (dependent on the distance to the transmitter) the RMS voltage of a received signal can be regarded as being constant. The signal fluctuations are caused by the Rayleigh distribution only. Measuring along runs over greater distances the RMS value changes slowly. This effect leads to a superimposed long term fading. Measured ensembles of a voltage with a long term changed Rayleigh fading show additional curvatures in the representation of Fig. 5.

4.22 Autocorrelation of the Electric Fieldstrength in a Rayleigh distributed Field

Following /4/ the spatial distributed autocovariance function for the E-field envelope in Rayleigh distributed fields

is given by the expression

$$R\ (d,\lambda_o) \approx I_o^{\,2}\ (2\pi \frac{d}{\lambda_o}) \qquad (10)$$

where I_o is the zero order Bessel function, d is the linear distance between two points within the field, and λ_o is the free space wavelength of the actual frequency. Equ.(10) is valid for vertical polarization of the E-field and plane grounds.

If one assumes a correlation factor of

$$R \leqslant 0.5 \qquad (12)$$

to be sufficient for a nearly optimum diversity gain equ. (10) requires a distance of

$$d \geqslant \lambda_o/6 \qquad (13)$$

Fig. 6 describes equ. 13 for the frequency range of 30 through 300 MHz. It points out that sufficient diversity should be possible in the whole frequency range with the available distances on a car if the car does not influence the field distribution too much. To verify the latter assumption extensive measurements of the covariance function for different antenna combinations have been accomplished over the full frequency range from 30 through 300 MHz. These measurements are described in chapter 5.1.

4.23 Diversity Systems

There are three basic diversity systems using two or more

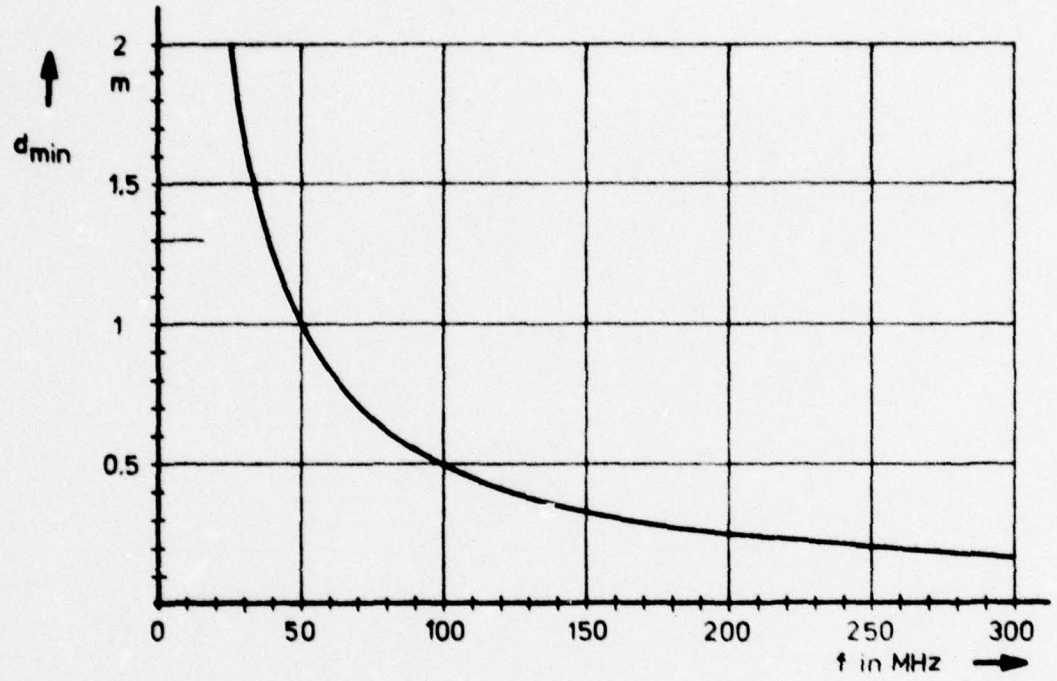

Fig. 6: Required minimum distance d_{min} for a correlation factor R ≤ 0.5 in Rayleigh fields over a plane ground

antennas /25/:

- selection diversity
- maximum ratio diversity
- equal gain diversity

In a selection diversity system always that antenna with the higher actual output voltage (or signal-to-noise ratio S/N) is connected to the receiver. In the maximum ratio diversity system the signals are weighted and then summed. The signal with the highest output voltage (or highest S/N) is considered strongest, the weaker signal is attenuated before being added. The equal gain system adds all signals without consideration of the actual RMS (or S/N) of the different branches.

The second and third system may operate in two different ways: The signals can be added coherently by cophasal summing in the RF- or IF-section or can be added by summing up after demodulation. The coherent method may achieve an improvement in the signal-to-noise ratio over the other systems if the signal is added in the RF section before the first amplifier stage with the help of noiseless phaseshifters. This improvement is less than 3 dB and requires a very sophisticated technique.

The diversity gain which can be obtained depends on the system in use, the lower detectable signal limit, the ratio of the RMS values of the diversity branches, and the correlation of the output voltages of the different antennas. The influence of these parameters is very complicated but solved in the literature (especially /8/, /25/, /26/, /27/).

As an example the diversity gain of a system with equal RMS values of both antennas using selection diversity is given in Fig. 7 in terms of the cumulative probability function. The curve for R = 1 is identical with the single Rayleigh distribution. If some examples are compared with the Rayleigh distribution, which is the same as the envelope probability of a single antenna in a Rayleigh field, one recognizes:

The signal is below the level - 20 dB (0 dB $\hat{=}$ V_m) during:

0.7	percent of time in the Rayleigh case	R = 1
0.02	percent of time for	R = 0.6
0.005	percent of time for	R = 0

The decrease of the non-availability below the - 20 dB level is a factor of 35 in the case of R = 0.6 and of 140 in the case of R = 0.

Or in terms of equal cumulative probability:

During 1 % of the time the signal is below

- 18 dB in the Rayleigh case
- 10 dB in the case of R = 0.6
- 8 dB in the case of R = 0

The latter comparison leads to the result that nearly the full diversity gain is achieved with correlation factors as small as about 0.5 through 0.7.

All other diversity systems show similar behaviour concerning the absolute values of the diversity gain and the dif-

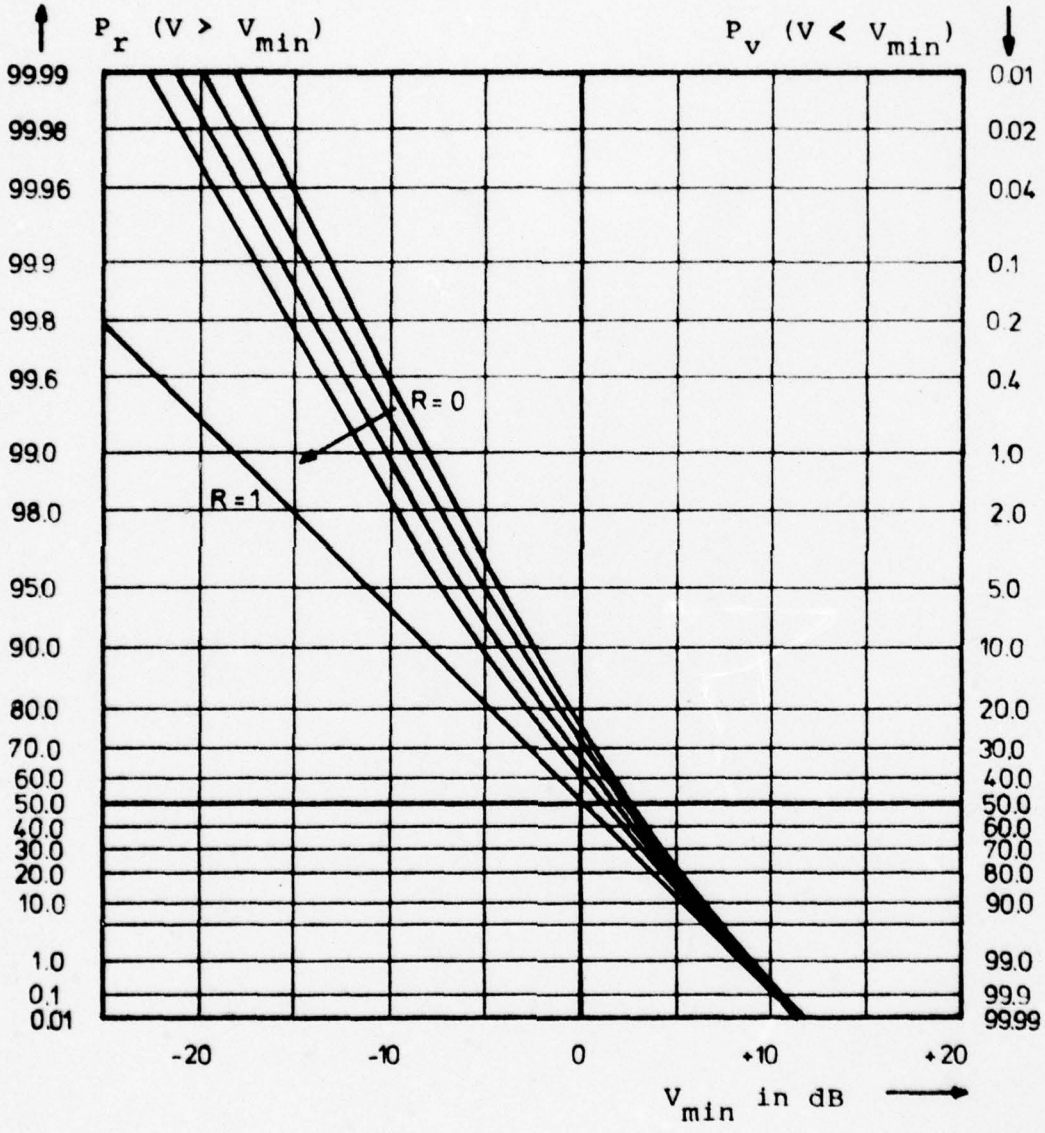

Fig. 7: Cumulative probability distribution for selection diversity and correlation factors of 0, 0.3, 0.6, 0.8, and 1.
(calculated after Brennan /27/)

ferences dependent on the correlation factor. On this account the evaluation of the following measurements have been done only for two systems, the selection diversity and the equal gain diversity.

5. Measurements of Cross Covariance Functions and Diversity Gains

The key problem of space diversity systems is the correlation factor of the output voltages of different antennas. Theoretically, assuming the plane ground, the dimensions of a car are sufficient large to promise a nearly optimum diversity gain above 30 MHz. The only question is the order of magnitude of the influence of the car's conducting surface on the wave distribution.

Certain structures along the car could show resonances at special frequencies and could determine the reception quantities rather than the antennas themselves. These resonances of the car would increase the correlation factor of the antenna voltages and reduce the diversity gain.

This problem was not considered in recent papers. Only at fixed frequencies has the correlation factor been measured dependent on the linear distance of the antennas /11/. On this account we performed extended measurements of the covariance function and the diversity gain for various antenna combinations on a car.

Fig. 8 shows the spacing of the 6 antennas in use. The linear distances of all measured antenna combinations are listed in this figure. A photograph of the used car with the mounted antennas is given in Fig. 9. Because of the angle of view only 5 antennas can be seen in this picture.

All antennas are of a broadband active type with short passive rods with a length of 30 cm.

Fig. 10 shows the circuit diagram of the used transistor

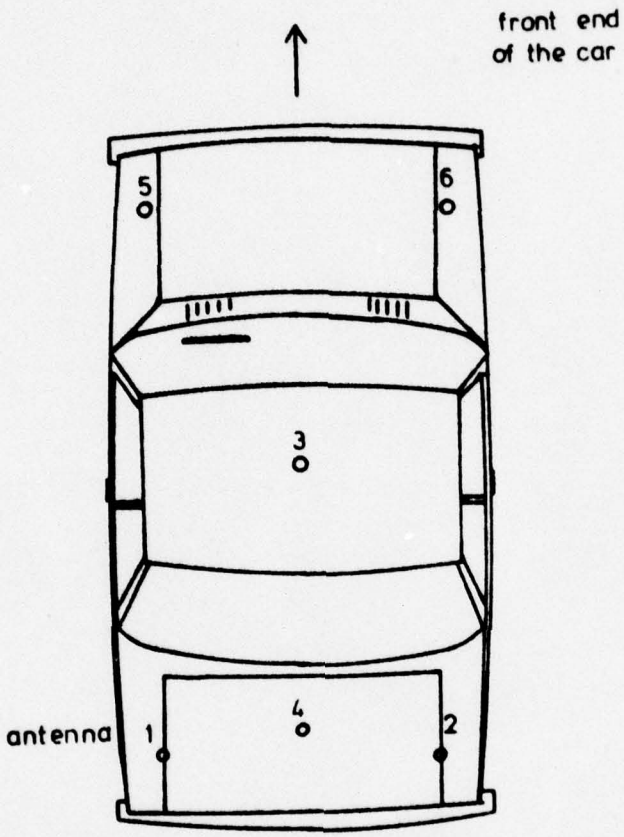

Linear distances d between the antennas

1-2	d	=	137 cm
1-4	d	=	70 cm
2-4	d	=	70 cm
5-6	d	=	124 cm
1-5	d	=	377 cm
1-6	d	=	394 cm
2-3	d	=	210 cm
4-6	d	=	372 cm
3-4	d	=	173 cm

Fig. 8: Antenna arrangement on the measuring car and linear distances between the single antennas of the 9 measured dual branch combinations.

Fig.9: Measuring car with five active broadband antennas mounted on various locations

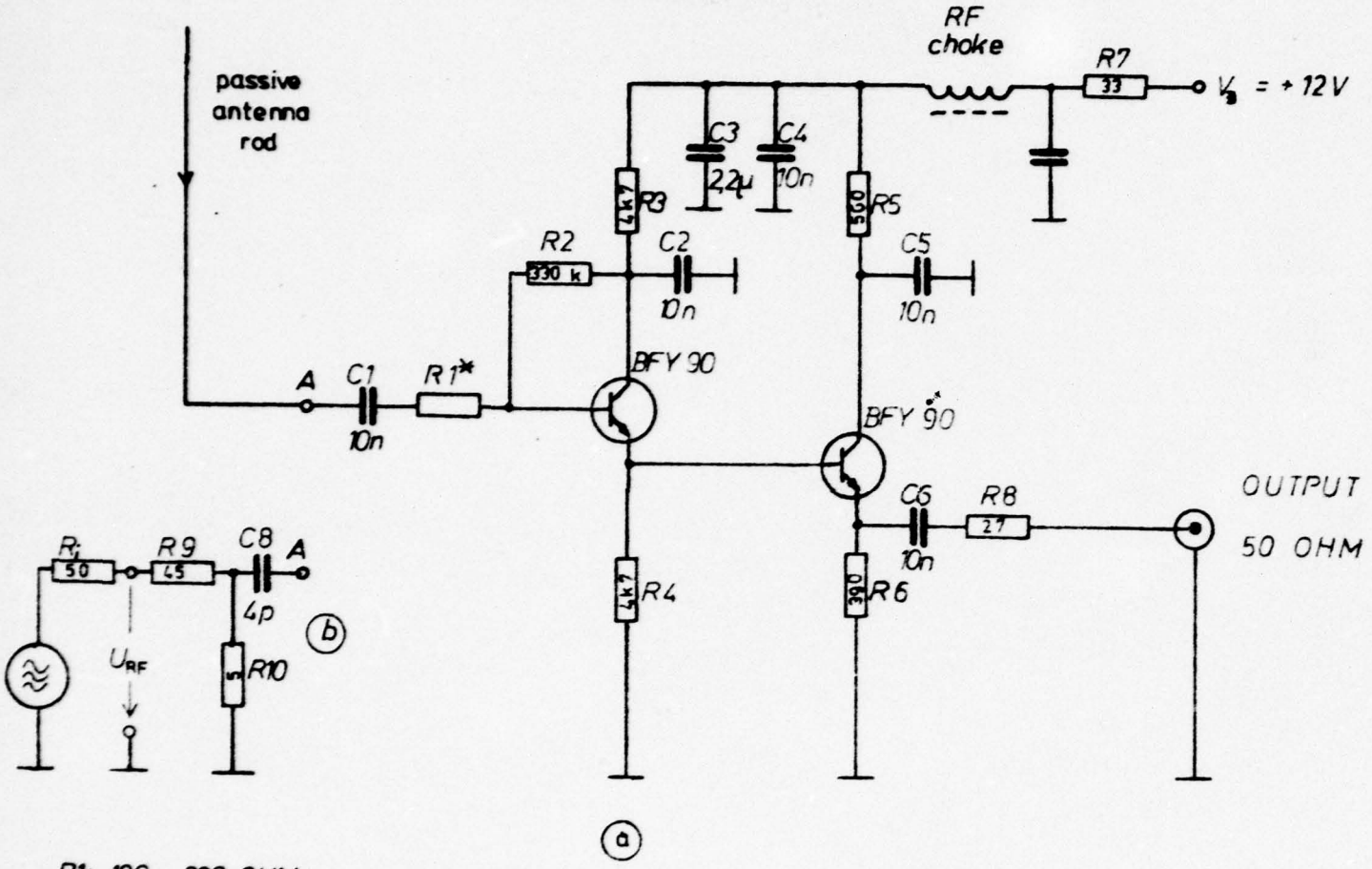

R1: 180...220 OHM

Fig. 10: a) Broadband transistorized receiving antenna for 30 ... 300 MHz
b) Equivalent circuit of the passive rod

amplifier which has low noise and a nearly constant gain behaviour within the frequency range of 30 through 300 MHz. This transistor amplifier is integrated in the antenna base.

The test assembly for the mobile receiption measurements is shown in Fig. 11. An AM transmitter with 1 W output and a reflectometer controlled matching box in connection with a vertically polarized transmitting antenna served as a base station. The location of the transmitting antenna was chosen in such a way that no direct wave could arrive at the receiving car during the test motion.

In the car three receivers of the type ESU 2 have been installed. The ESU 2 achieves a DC output voltage proportional to the magnitude of the RF input voltage over the wide dynamic range of about 40 dB. During each measuring drive three antenna output voltages could be measured and recorded due to the availability of the three test receivers. The simultaneous recordings were performed with the help of a 4-channel FM tape recorder. The 4^{th} channel was used for comments during the measuring drive, for instance the indication of a time interval with an externally forced stop.

We used an AM transmitter with a continuous 3 kHz modulation for the identification of the receiver tuning.

The evaluation of each tape record is possible for three two-branch diversity combinations. For evaluating nine combinations at nine different frequencies, at least 27 test drives are necessary. For redundancy we performed 37 drives, each drive with a time duration of 150 sec.

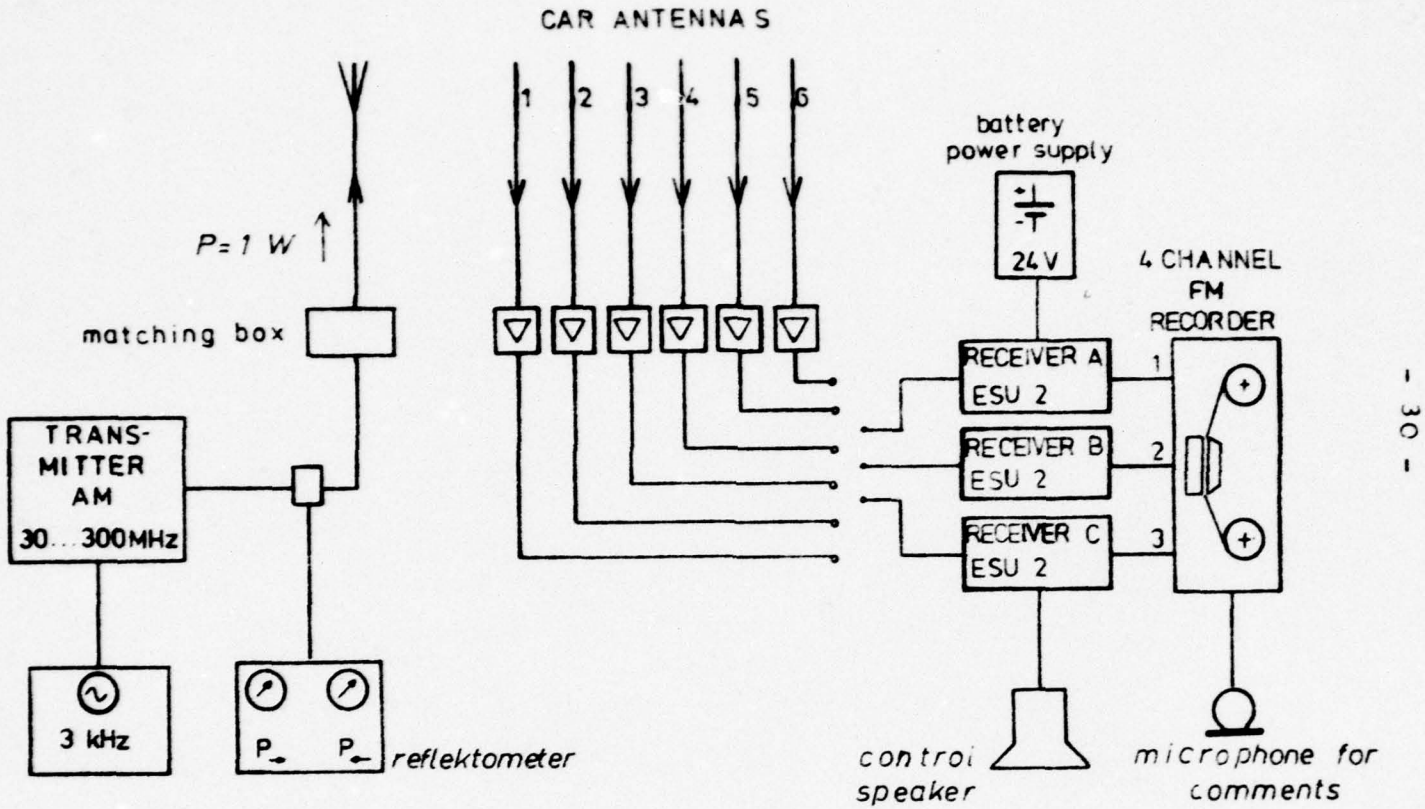

Fig. 11: Test assembly for the measuring drives

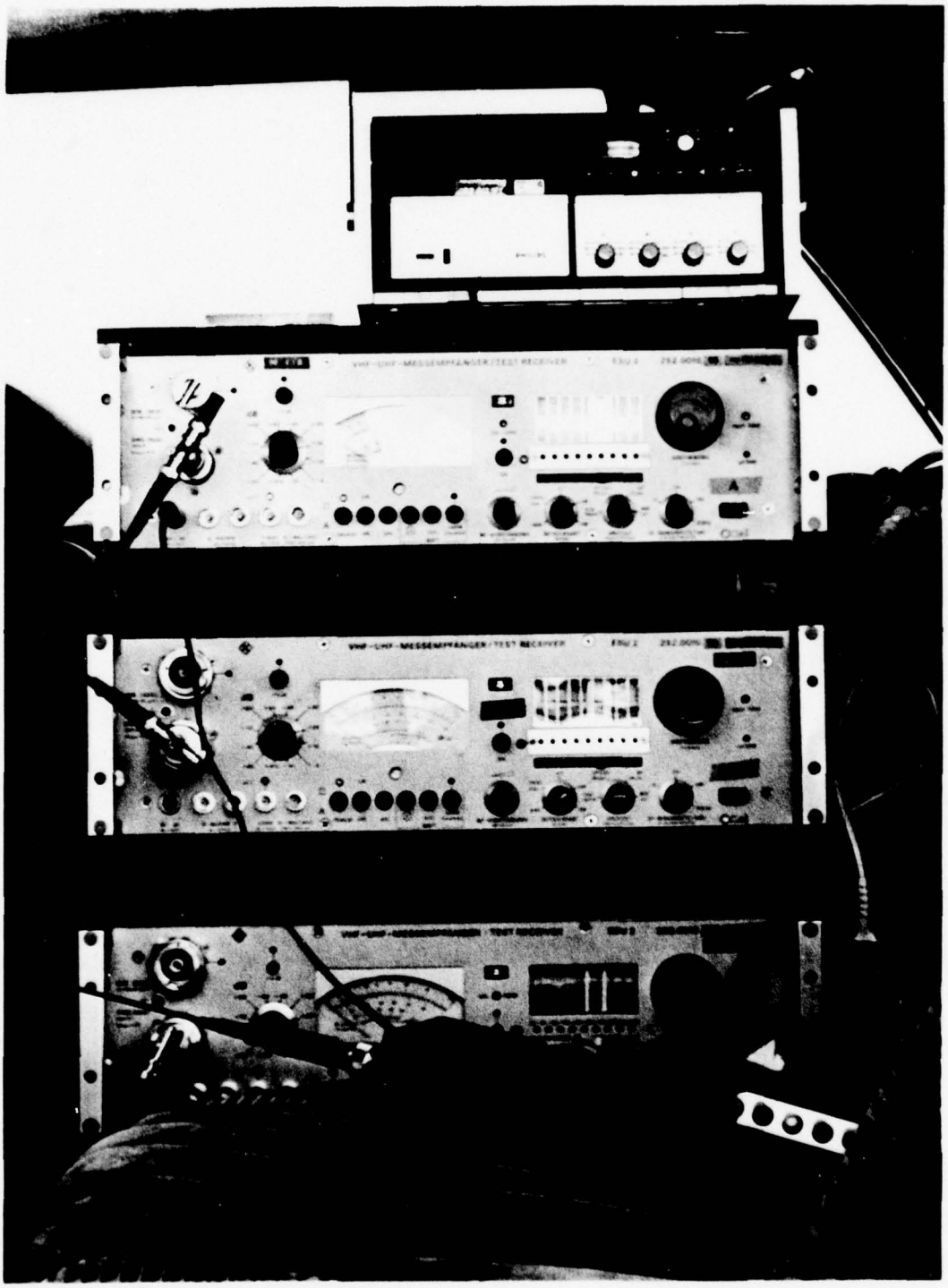

Fig.12: Three identical test receivers and FM-tape recorder in the car

5.1 Cross correlation

The circuit for the evaluation of the tape records is given in Fig. 13. Always two of three recorded tracks are selected and fed to the channels A and B of the evaluation circuit. After some processing of the analog tape recorder outputs the signals of both channels are A/D converted and picked up by the digital calculator. The final evaluation is performed by digital computer means.

The sampling rate of our computer is 7 Hz. The power spectrum of the recorded antenna output voltages is extended up to about 10 Hz due to the chosen speed of 10 mph for the test drive and the measured frequencies. To get a sufficiently high sampling rate we decreased the speed of the tape recorder by a factor of 10 during the evaluating playback. On this account we get an effective sampling rate of 70 Hz. The correlation factor of the two channel output voltages is

$$R = \frac{\overline{(V_A - \overline{V_A})\ (V_B - \overline{V_B})}}{\sqrt{\overline{(V_A - \overline{V_A})^2} \cdot \overline{(V_B - \overline{V_B})^2}}} \qquad (14)$$

where V_A is the output voltage of channel A and V_B is the output voltage of channel B. The dash expresses a time averaging.

If the results should be compared with the theoretical results of the Rayleigh fading one has to take into account that the averages $\overline{V_A}$ and $\overline{V_B}$ are valid only for restricted extension of the test drive. At longer test drives $\overline{V_A}$ and $\overline{V_B}$ show a slow long term fading dependent on the medium

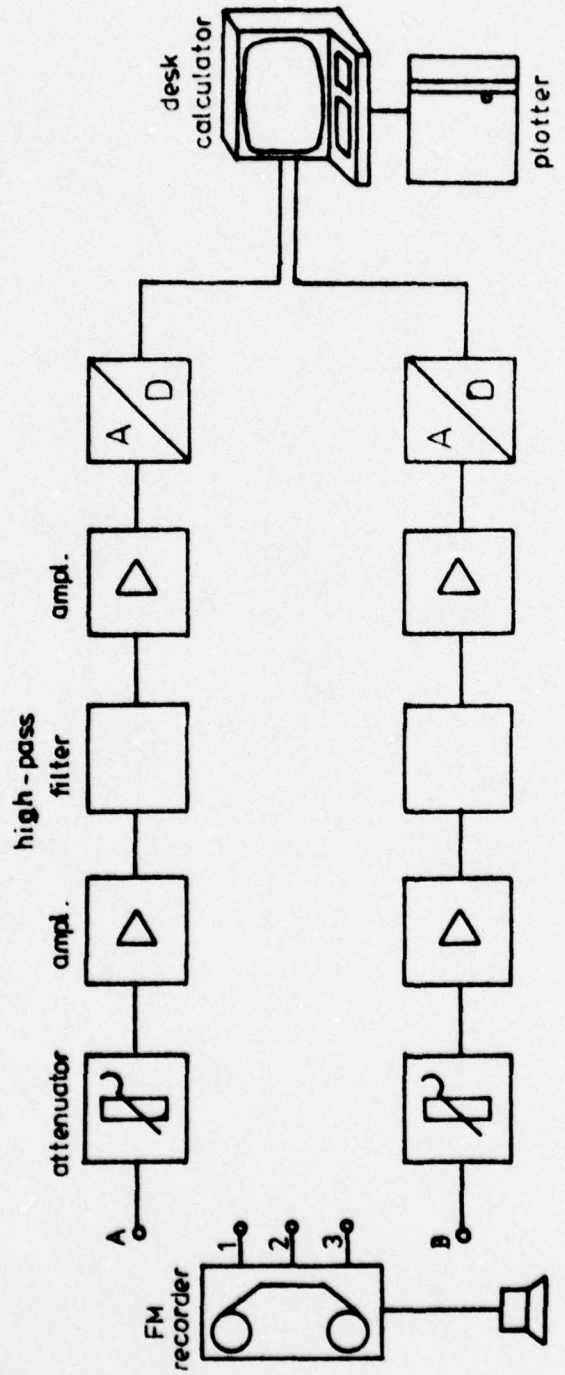

Fig. 13: Record evaluation circuit

power arriving at the different areas passed during the drive. On this account we restricted the averaging of V_A and V_B to driven distances of about 25 meters or about 5 sec of the output voltage records. The differences $V_\nu - \overline{V_\nu}$ in equ. 14 are produced with the help of analog high-pass filters in the amplifier channels of Fig. 13. The principle of this filter is shown in Fig. 14.

The time constant is chosen to be $\tau = 50$ s which acts as a time constant of 5 s related to real time.

The computer program is written in BASIC and is described in the appendix.

The obtained results are given in Fig. 15 through 22 assorted for increasing linear distance d between the antennas. For a comparison to the theoretical results for antennas over a plane ground we draw the square of the zero-order Besselfunction $J_o^2\ (2\pi\ ^d/\lambda_o)$ as a dashed line in all these figures. Although the correlation factors have been measured only at discrete frequencies we connected the measured values to a polygonal covariance function. The purpose is only a clearer representation of the results. Of course, we suppose a more complicated micro structure between the measured points. A future scientific project of our group will be the measurement of a covariance function with much closer measuring points to get even the fine structure.

Fig. 15 compares the two antenna couples 1-4 and 2-4, respectively. Both antenna pairs have equal distances and are symmetrically mounted one to another. Due to these conditions the results should be identical. The differences which we obtained between the circles and the crosses in Fig. 15 demon-

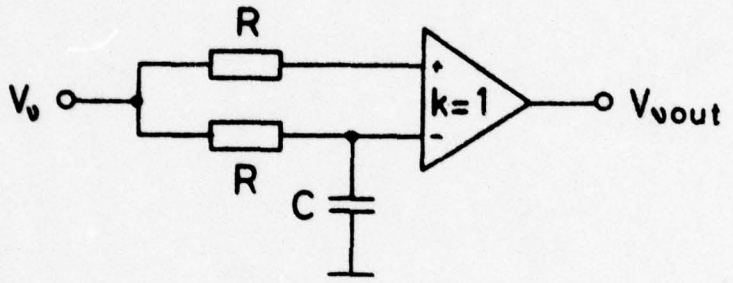

$$\tau = R \cdot C$$

$$V_{vout} \approx V_v - \frac{1}{\tau} \int_{t-\tau}^{t} V_v \cdot dt$$

$$\approx V_v - \overline{V_v}$$

Fig. 14: High-pass filter for the elimination of the linear average

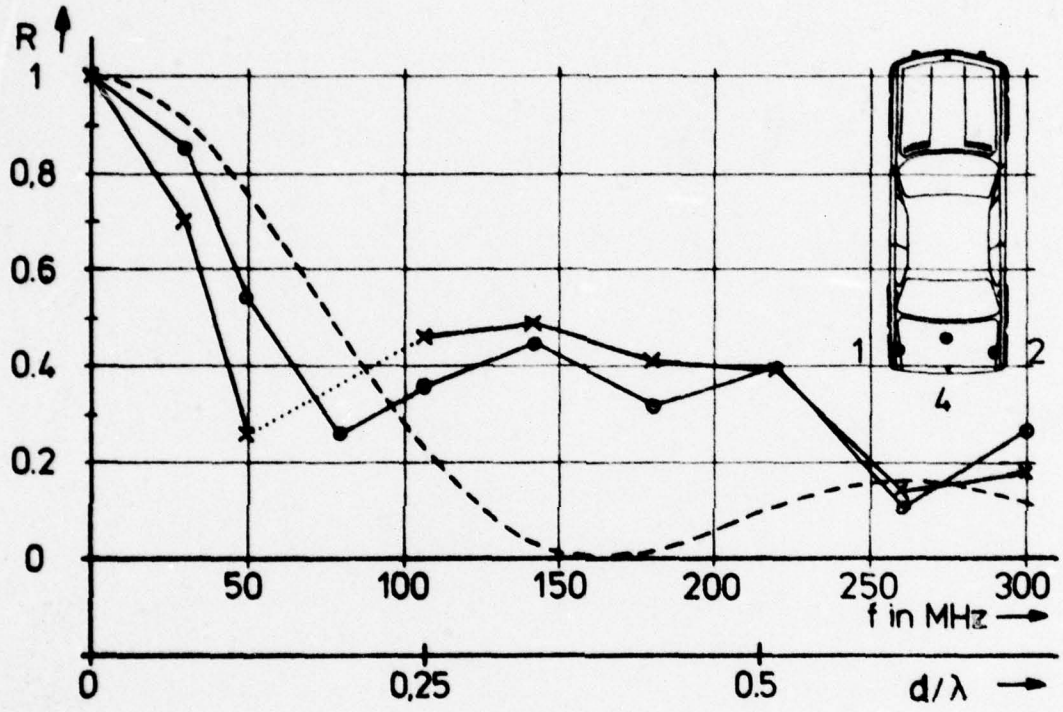

Fig. 15: Covariance function R of the output voltage envelopes of antennas 1-4 and 2-4

x = 1-4

O = 2-4

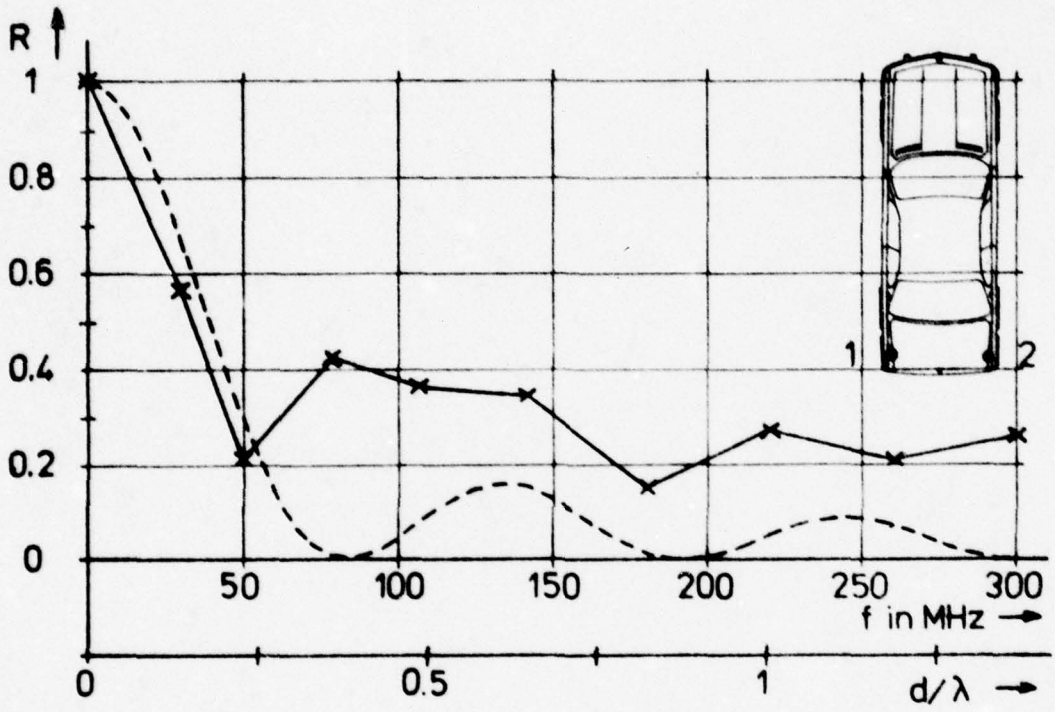

Fig. 16: Covariance function R of the output voltage envelopes of the antennas 1 and 2

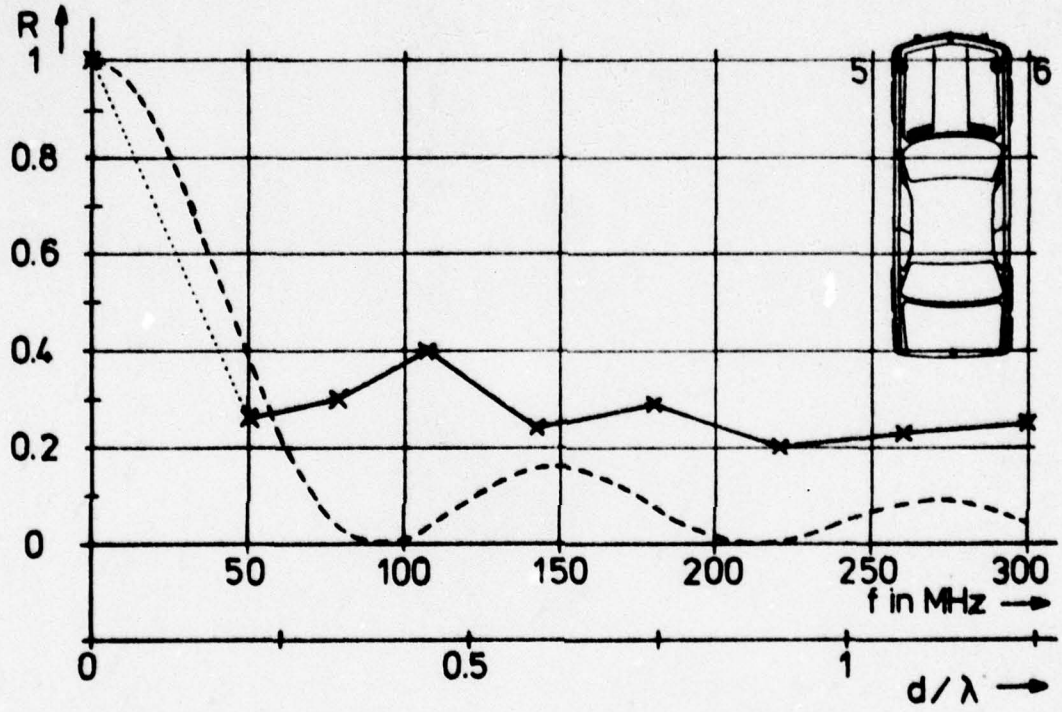

Fig. 17: Covariance function R of the output voltage envelopes of the antennas 5 and 6.

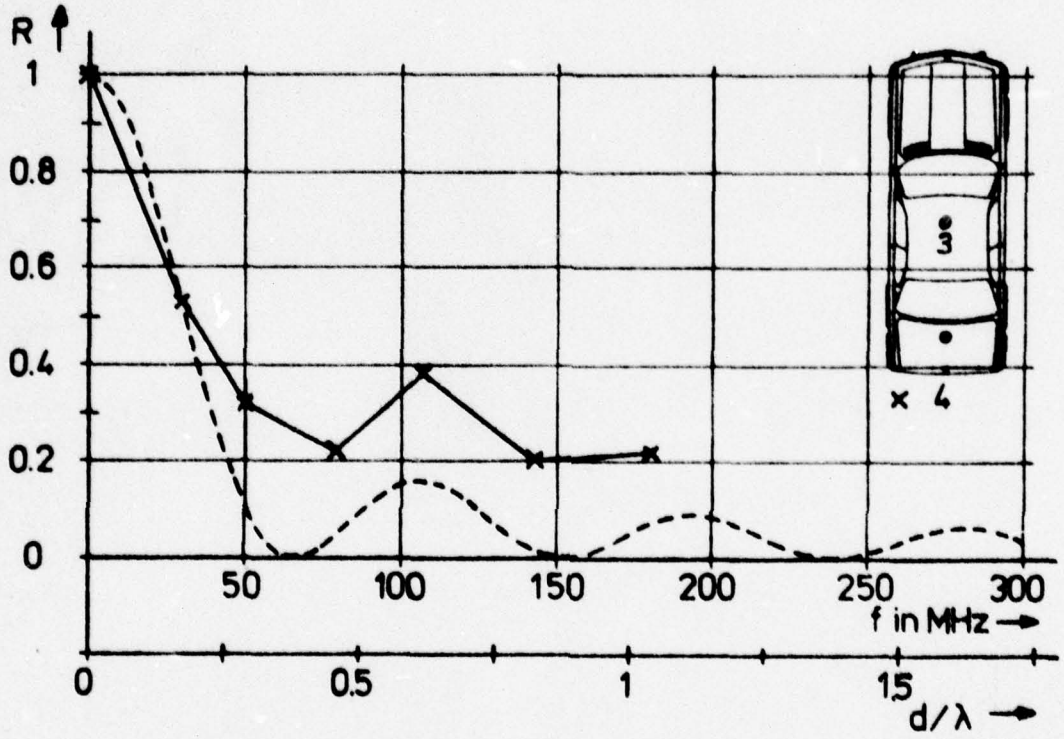

Fig. 18: Covariance function R of the output voltage envelopes of the antennas 3 and 4

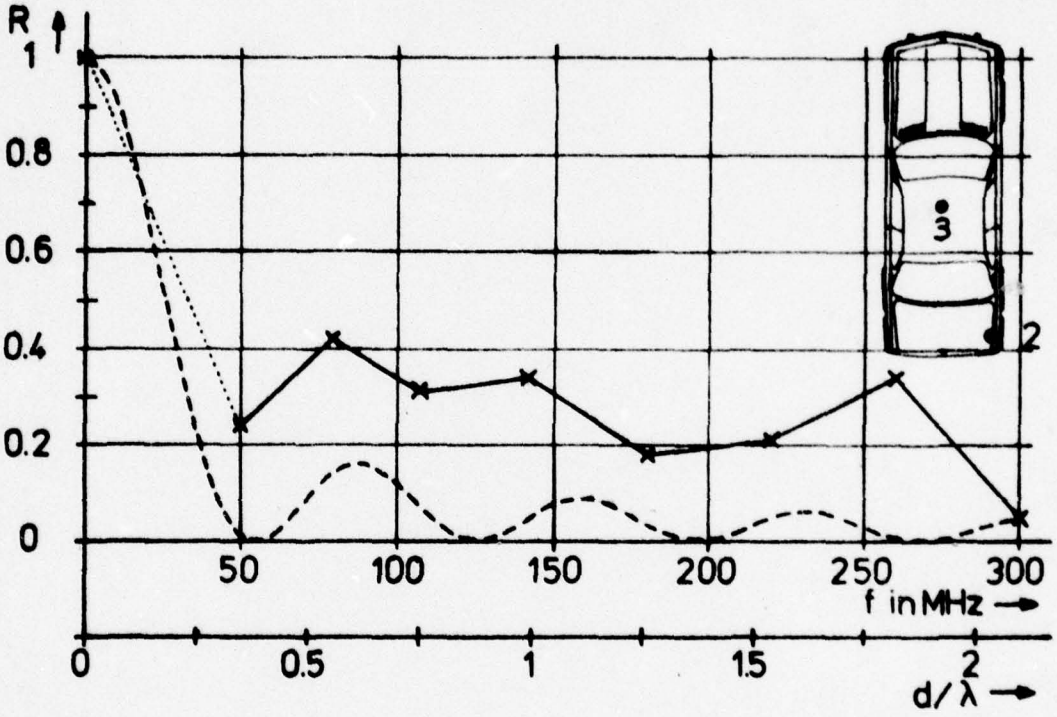

Fig. 19: Covariance function R of the output voltage envelopes of the antennas 2 and 3

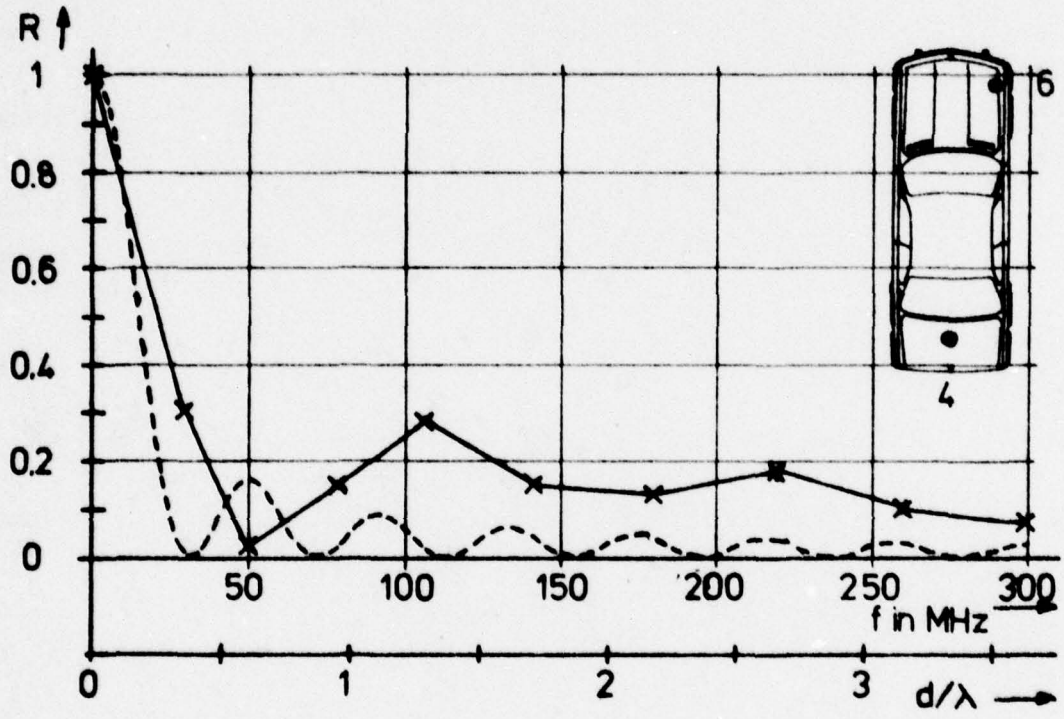

Fig. 20: Covariance function R of the output voltage envelopes of the antennas 4 and 6

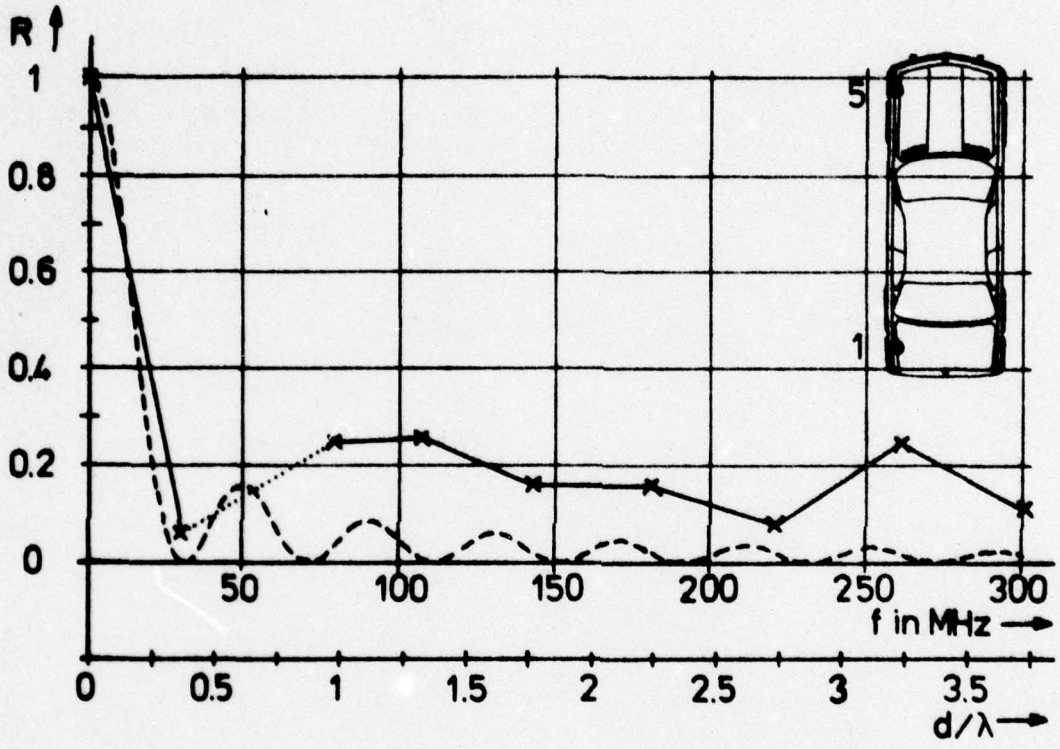

Fig. 21: Covariance function R of the output voltage envelopes of the antennas 1 and 5

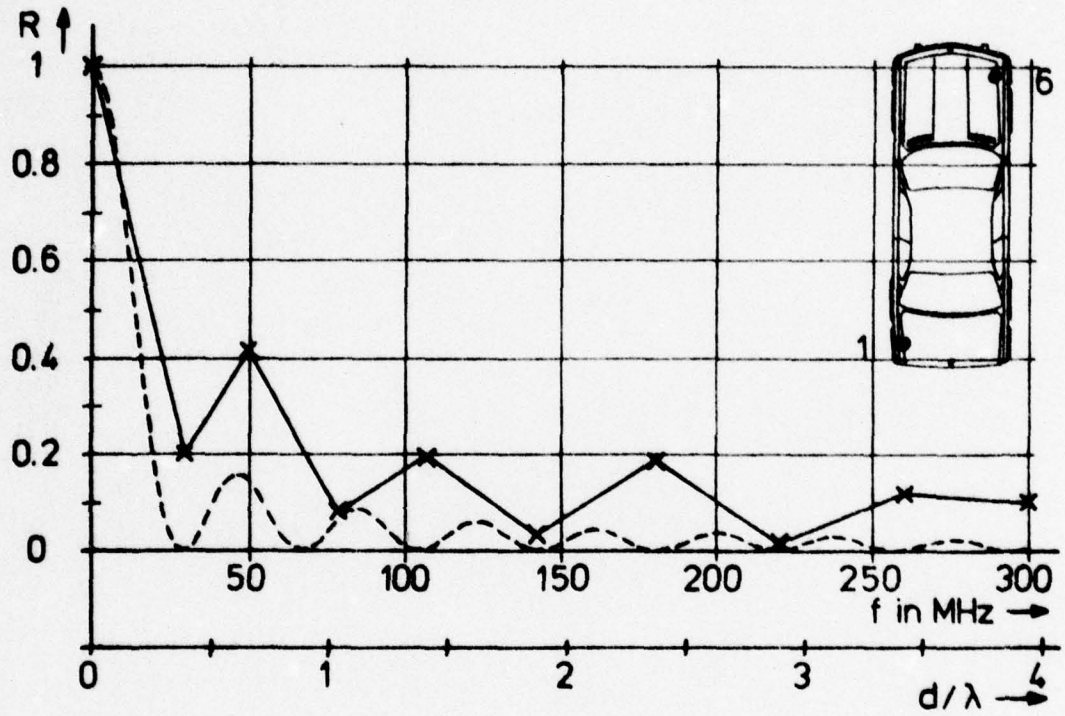

Fig. 22: Covariance function R of the output voltage envelopes of the antennas 1 and 6

strate the order of accuracy of our measuring method. At the lowest frequencies of 30 and 50 MHz the differences of both results are higher. In this region the number of reflections seems to be lower and the results depend on the driving course and the direction between transmitting antenna, measuring site, and driving direction more than at higher frequencies. With increasing frequency more reflected waves seem to be existent. The dependence on the side of the car where the antennas are mounted decreases and the differences of the results become smaller.

The comparison of the results in Fig. 15 to the theoretical covariance function for antennas over a plane ground shows an obvious increase of the correlation due to the influence of the car, especially at higher frequencies. At lower frequencies the correlation is smaller than the theoretical value. If one assumes values of $R \ll 0.5$ to be sufficient for an adequate diversity gain the lower frequency limit is about 50 MHz for this antenna distance.

Fig. 16 describes the antenna combination 1-2. This antennas show a sufficient decorrelation even at the lowest frequency of 30 MHz. The symmetrically mounting of this antennas perhaps leads to a better similarity to the theoretical covariance function. But, the increase of correlation is obvious, too.

The figures 17 through 22 show a decrease in the correlation with increasing distance d. The maximum possible distance along the car is used by the antenna combination 1-6. In this case the correlation factor is as small as 0.2 even at the lowest measured frequency of 30 MHz. Only at 50 MHz this value is exceeded to a level of R = 0.4. At all other frequencies the correlation is below the value of 0.2, too. Al-

though the covariance nearly at all frequencies is higher than in the theoretical case this antenna combination shows best performance for space diversity systems above 30 MHz.

As a comprehensive result one recognizes that all antenna combinations show correlation factors below R = 0.5 for frequencies above 30 MHz. The only exceptions are the very close combinations 1-4 and 2-4 at frequencies below 50 MHz. To show this result Fig. 23 and 24 represent composite drawings of all results dependent on the relative distance d/λ_o and dependent on frequency, respectively.

5.2 Diversity Gain - Fade Reduction

The diversity gain of a two branch system approximately can be calculated if both output voltages are Rayleigh distributed and if the correlation factor of both voltages and the ratio of the RMS values of both antennas are known. Furthermore, in the literature equal noise power N in both channels is assumed, which is true in the case of negleqable outer noise, i.e. when the receiver noise is the major component. Under these conditions following Vigants /8/ the fade reduction factor F for the selection diversity, for example, can be calculated:

$$F = \frac{P_r(S_2/N < S_{min}/N)}{P_r(S_2/N < S_{min}/N,\ S_1/N < S_{min}/N)} \qquad (15)$$

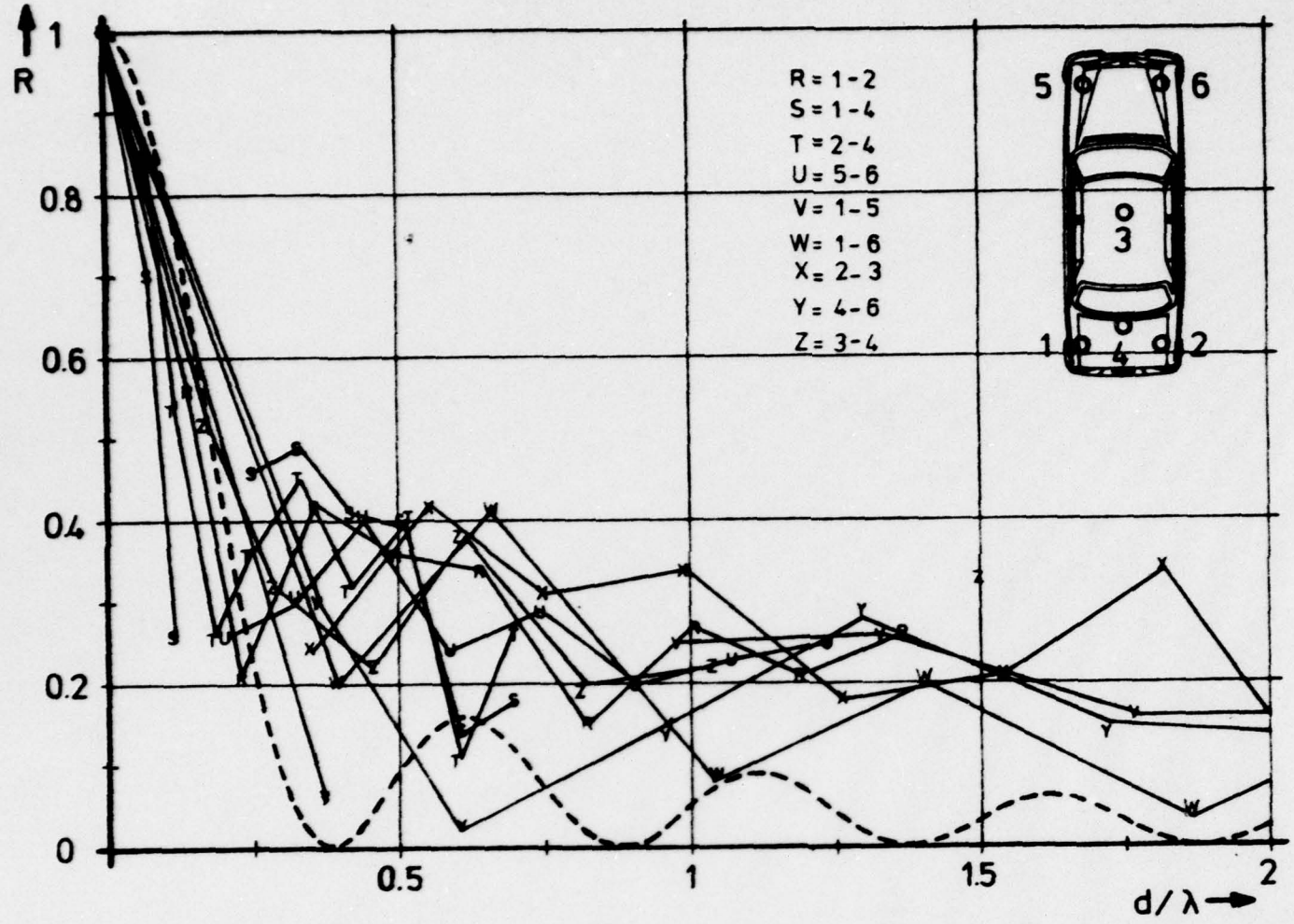

Fig. 23: Covariance functions R of all measured antenna combinations dependent on d/λ_o

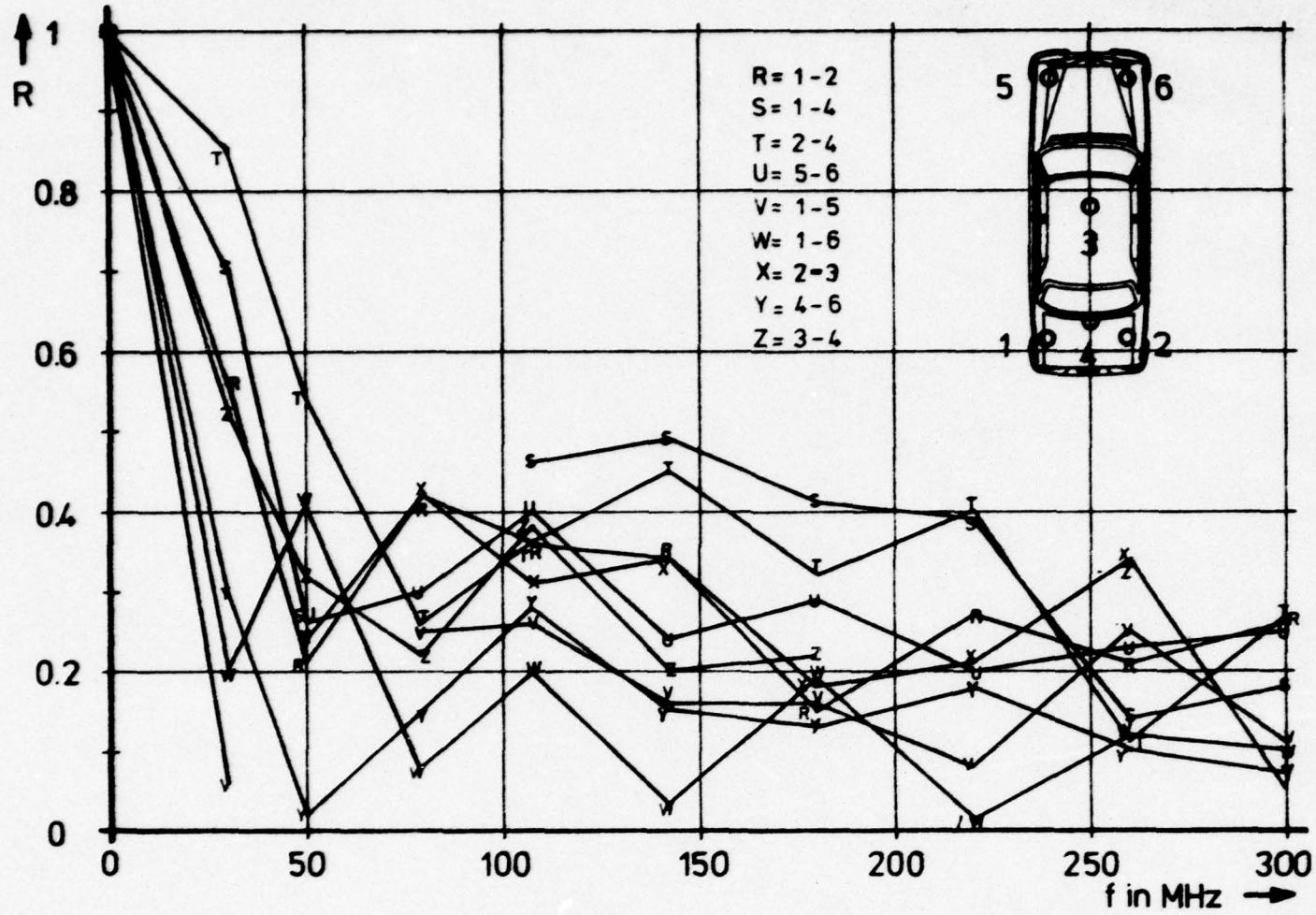

Fig. 24: Covariance functions R of all measured antenna combinations dependent on frequency

$$F \approx (1-R)\ \frac{\overline{V_1^2}/\overline{V_2^2}}{V_{min}^2/V_2^2}\ \Bigg|_{V_{min} \ll \sqrt{V_2^2}} \qquad (16)$$

(N = noise power,
S_1 = signal power of channel 1, S_2 = signal power of channel 2, S_{min}/N = actual S/N threshold,
V_1^2 = RMS of antenna 1, V_2^2 = RMS of antenna 2,
V_{min} = threshold voltage belonging to the S/N threshold,
R = correlation factor)

The fade reduction factor expresses the ratio of the probabilities that the S/N in one channel is below a certain level S_{min}/N and that the S/N in both channels simultaneously is below the same level, respectively. The higher the fading reduction factor F is, the higher is the advantage of the diversity system.

The approximate solution of equ. 15 which is given in equ. 16 depends on the correlation factor, the ratio of the RMS values of both channels and the chosen threshold V_{min}.

On the other hand the fade reduction of diversity systems can be solved numerically with the help of computer methods since the results of the test drives are stored on the magnetic tape. We started to evaluate the test drives under this point of view, but, the evaluation is not finished until now. As an example the results of the antenna combination 1-2 for the frequencies 30 MHz and 220 MHz are given in the following.

The evaluation of the fade reduction factor has been performed for the selection diversity and the equal gain diversity (other diversity systems show only minor differences to the two regarded systems). We used the same equipment as sketched in Fig. 13 but without the dynamic average elimination circuit of Fig. 14. The calculator accumulates the results of the 4 checks

$$V_A > V_{min} \longrightarrow \text{antenna A}$$

$$V_B > V_{min} \longrightarrow \text{antenna B}$$

$$V_A > V_{min} \text{ or } V_B > V_{min} \longrightarrow \text{selection diversity}$$

$$(V_A + V_B) > \sqrt{2} \cdot V_{min} \longrightarrow \text{equal gain diversity}$$

for each sample of the measured voltages V_A and V_B and for various threshold values V_{min}. The results are the cumulative distributions for the antenna voltages themselves, the selection diversity, and the equal gain diversity, respectively.

Since the noise power is assumed to be identical in all channels the results can be normalized to signal/noise ratios. The final results for the evaluated measurements are shown in Fig. 25 for f = 30 MHz and in Fig. 26 for f = 220 MHz. The standard value in both figures is the median signal/noise S_{m2}/N which is exceeded in 50 % of the time by the output voltage of antenna 2. S_{min}/N is the varied threshold of the signal/noise ratio.

At 30 MHz the median voltages of both antennas differ 6.1 dB, antenna 1 being the weaker one. The Rayleigh distribu-

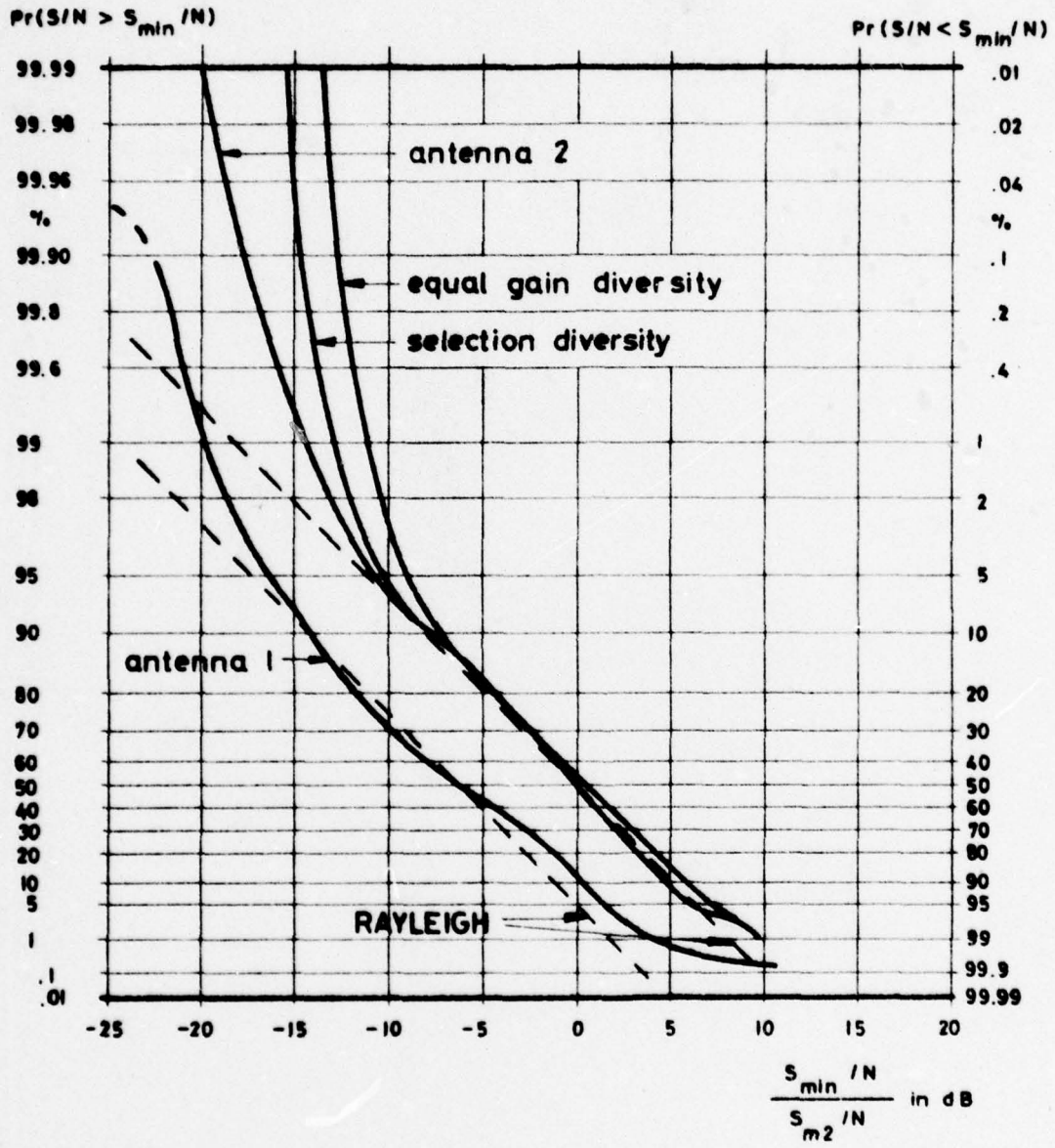

Fig. 25: Cumulative probabilities for the S/N for antenna 1, antenna 2, selection diversity, and equal gain diversity.

S_{min}/N = variable threshold

S_{m2}/N = standard S/N, which is exceeded in 50 % of the time by antenna 2

f = 30 MHz, antennas 1 and 2

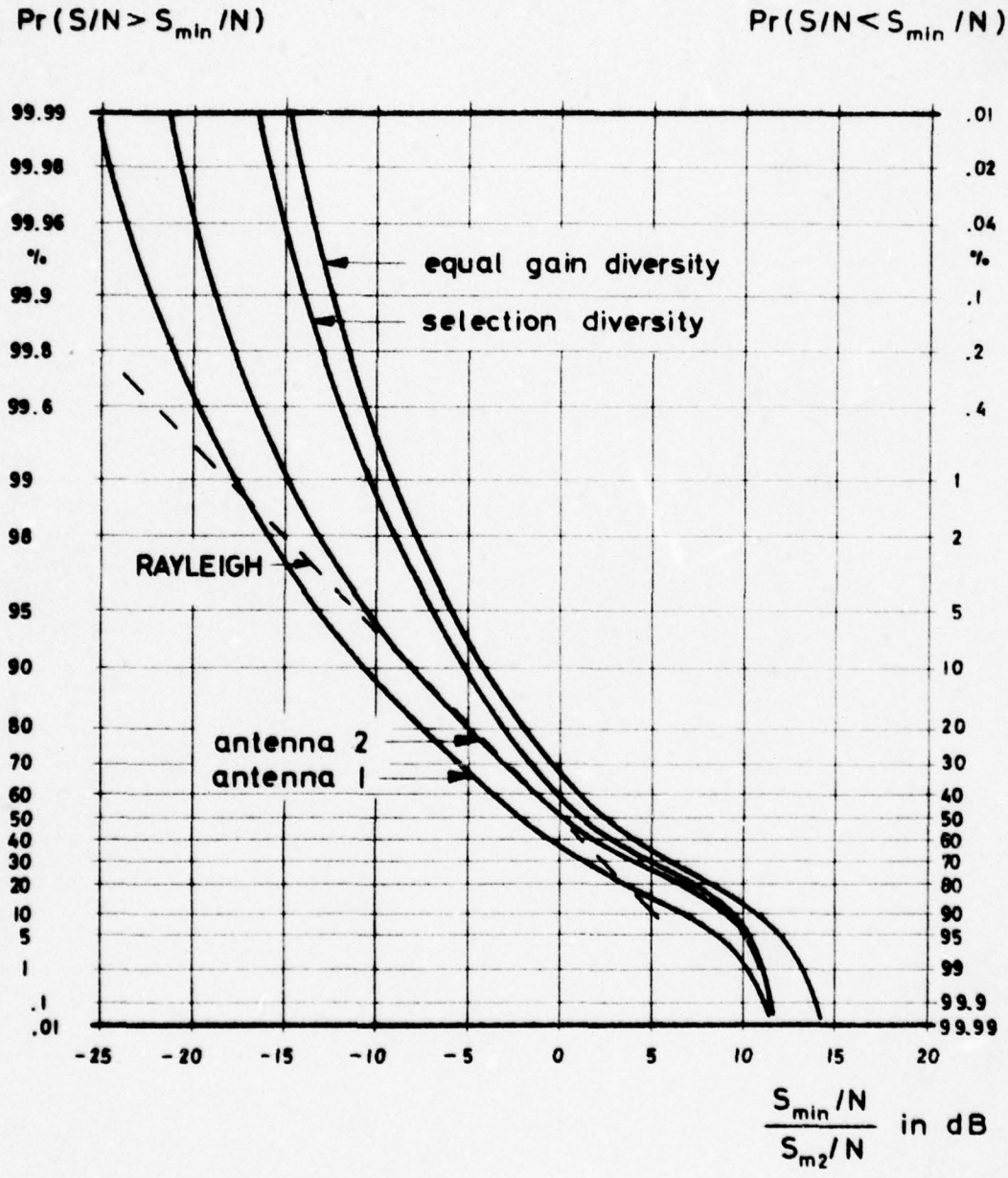

Fig. 26: Cumulative probabilities for S/N for antenna 1, antenna 2, selection diversity, and equal gain diversity.

S_{min}/N = variable threshold

S_{m2}/N = standard S/N, which is exceeded in 50 % of the time by antenna 2

f = 220 MHz, antennas 1 and 2

tion is approached within $\pm$ 1 dB over a dynamic range of about 15 to 20 dB. Because of the obvious difference of the RMS output voltages both the selection diversity as well as the equal gain diversity system become effective below about - 10 dB compared to the median signal/noise ratio S_{m2}/N of the stronger antenna 2.

At 220 MHz, Fig. 26, the difference of both antennas at the median level is 2.2 dB, antenna 2 being the stronger one again. The Rayleigh distribution is approached within $\pm$ 1 dB over a dynamic range of about 15 dB by both antennas. As the difference of both antennas is less compared to 30 MHz the diversity gain becomes effective even for higher threshold values.

The fade reduction factor F can be read out of Figs. 25 and 26 for each threshold level. For the selection diversity system the readings for 0 dB, - 5 dB, - 10 dB, - 15 dB, and 17.5 dB are shown in Fig. 27. For a comparison the theoretical results of equ. 16 which are valid for deep fades ($V_{min}^2 \ll \overline{V^2}$) only are shown, too. Especially at 220 MHz an obvious accordance between the numerically calculated results using measured data and the theoretical values can be observed. For the theoretical asymptotes in Fig. 27 the following data were used to calculate equ. 16:

<u>30 MHz</u>

$R = 0.57$ from Fig. 16

$\overline{V_1^2}/\overline{V_2^2} \approx V_{m1}^2/V_{m2}^2 = -6.1$ dB from Fig. 25

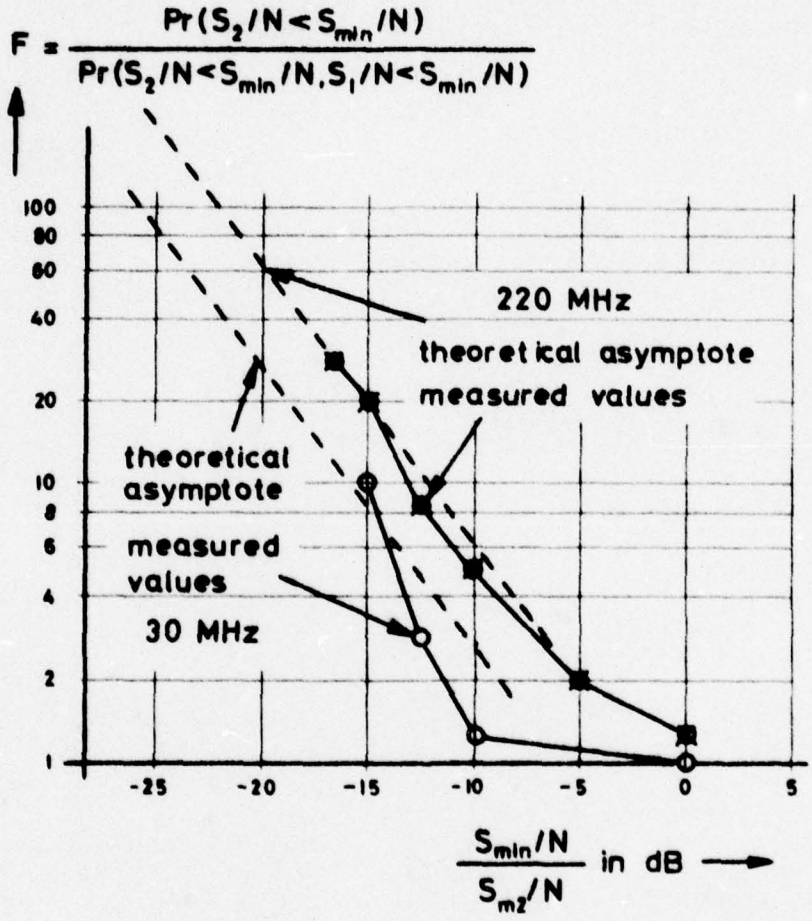

Fig. 27: Fade reduction factor F depending on the threshold level for antenna combination 1-2 and the frequencies f = 30 MHz and f = 220 MHu.
Measured values and calculated asymptote for deep fades.

220 MHz

$\underline{R} = \underline{0.28}$ from Fig. 16
V_1^2/V_2^2 $V_{m1}^2/V_{m2}^2 = -2.2$ dB from Fig. 26

Instead of the ratio of the RMS values we used the ratio of the median values V_{m1} and V_{m2} which could be determined with higher accuracy in our computerized evaluation circuit.

The results of Fig. 27 encourage to use the correlation factor R, which has been determined in chapter 5.1, and the ratio of the median values V_m of the output voltages to calculate the fade reduction of diversity systems. In spite of the certain differences of the measured antenna voltage distributions to the Rayleigh distribution the calculation accuracy seems to be sufficient concerning the reduction of the deep fades. Therefore, we will determine the ratios of the median output voltages for the other antenna combinations. The result obtained until now is given in Tab. 1 using antenna 2 with the maximum output voltage as a standard value of 0 dB.

f/MHz Antenna	30	50	79	107	142	180	220	260	300
1	-6.1	-3.6	-4.5	-1.1	-1.1	-1.7	-2.2	-1.2	-1.9
2	0	0	0	0	0	0	0	0	0
4	-3.6	-0.1	-1.5	-5.9	-2.8	-3.2	-4.4	-3.5	-2.4

Tab. 1: Median output voltages v_m in dB of the three evaluated antennas compared to the antenna with the maximum output voltage at the actual frequency.

6. Experimental Receiver

For experiments with various antenna spacings in the FM broadcast band we developed a postdetection two channel diversity receiver. This receiver will be delivered to ECOM for practical use.

Fig. 28 shows the principle of the receiver. Two separate tuners are fed from a common VCO as local oscillator to achieve an accurate tuning to the same receiving frequency. Both channels show separate IF amplifiers. The AFC voltages of both FM detectors are added to get sufficient AFC also in the case of one antenna being in a deep fade.

The audio signals are combined with the help of an integrated stereo balance controller. This combining circuit is driven by a differential amplifier which uses the "field-strength indicator" outputs of both IF amplifier. Thus the stereo balance controller weighs the audio output voltages: The output of the channel with the higher antenna voltage is weighed more strongly compared to the other. As long as both channels work above the limiting threshold the audio output voltage is constant and the receiver acts as a maximum ratio diversity system.

The maximum attenuation of the TCA 730 is high enough to fade out the noise of one channel with zero antenna voltage. The used audio amplifier IC can be switched to an automatic volume control.

Fig. 29 shows the circuit diagram and Figs 30 and 31 photographs of the receiver.

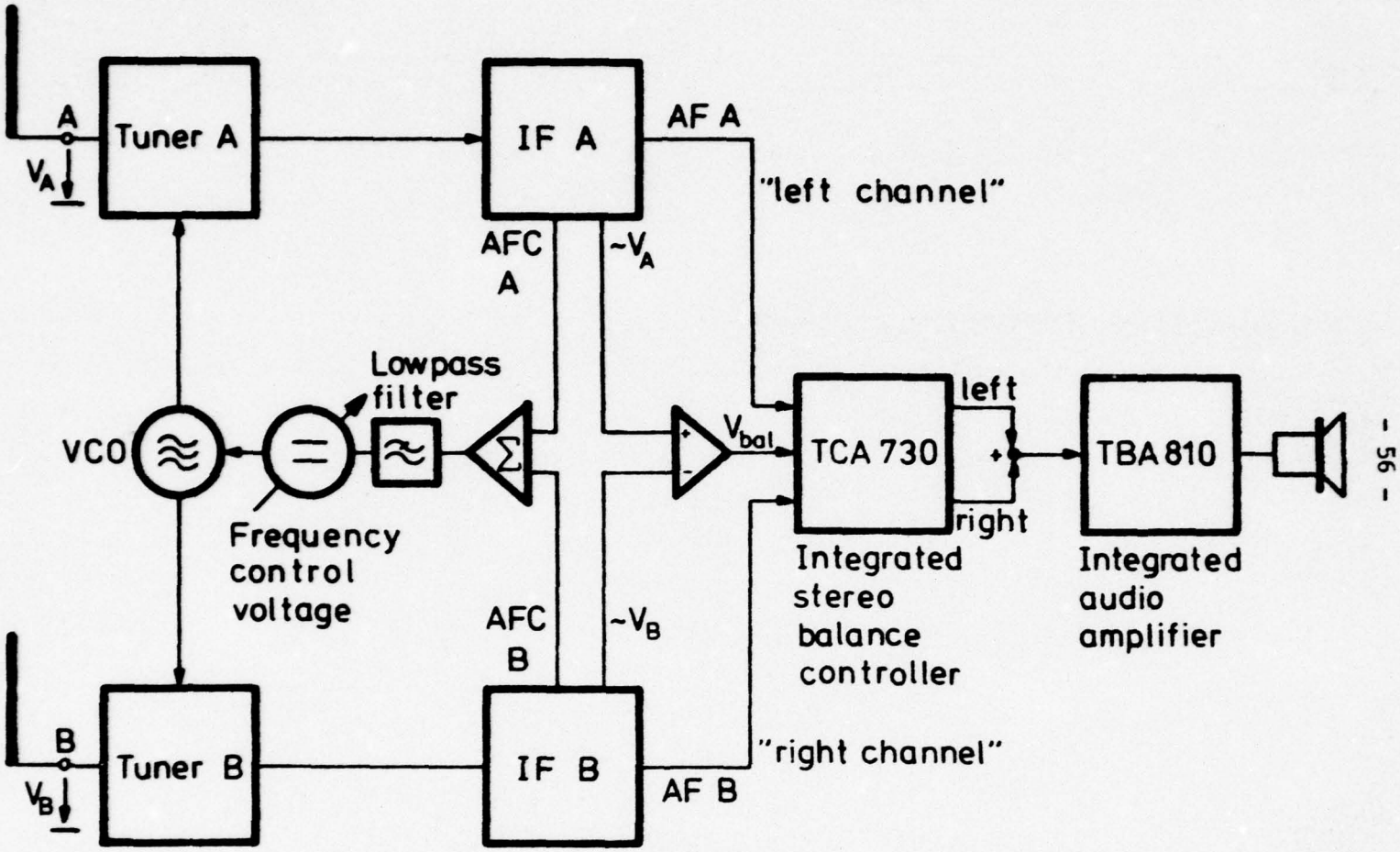

Fig. 28: Block diagram of a maximum ratio diversity receiver for the FM broadcast band

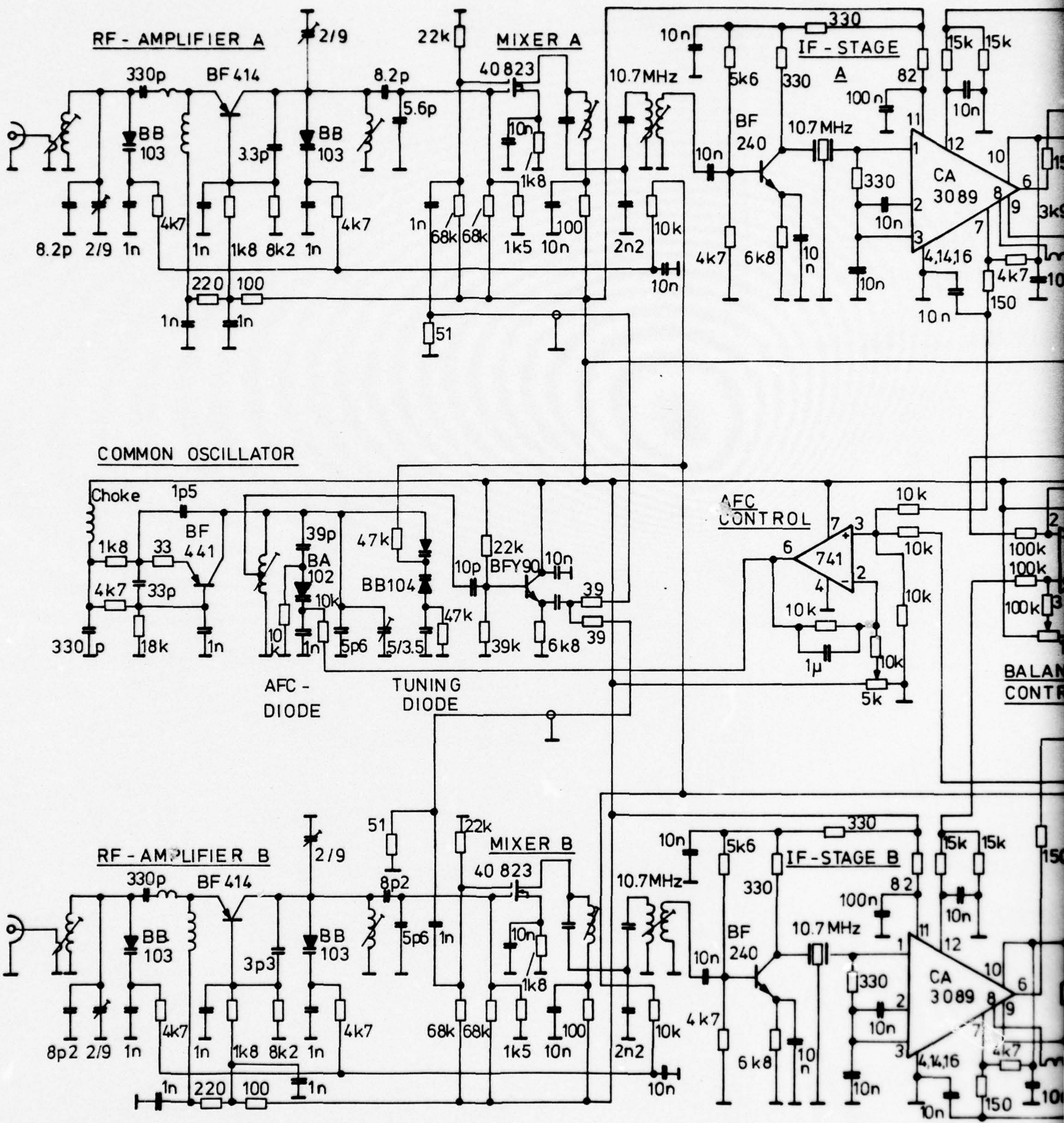
RF - AMPLIFIER A
BF 414
BB 103
330p
8.2p
5.6p
3.3p
2/9
MIXER A
40 823
22k
68k
1k5
1k8
10.7MHz
IF - STAGE A
BF 240
5k6
4k7
6k8
330
82
100 n
15k
CA 3089
2n2
10k
220
100
51
150
COMMON OSCILLATOR
Choke
1p5
BF 441
1k8
33
4k7
33p
18k
330 p
39p
BA 102
BB104
47k
10p
BFY90
22k
39k
6k8
39
5p6
5/3.5
AFC - DIODE
TUNING DIODE
AFC CONTROL
741
10k
100k
1μ
5k
BALAN
CONTR
RF - AMPLIFIER B
MIXER B
IF - STAGE B
8p2
3p3
5p6
4,14,16

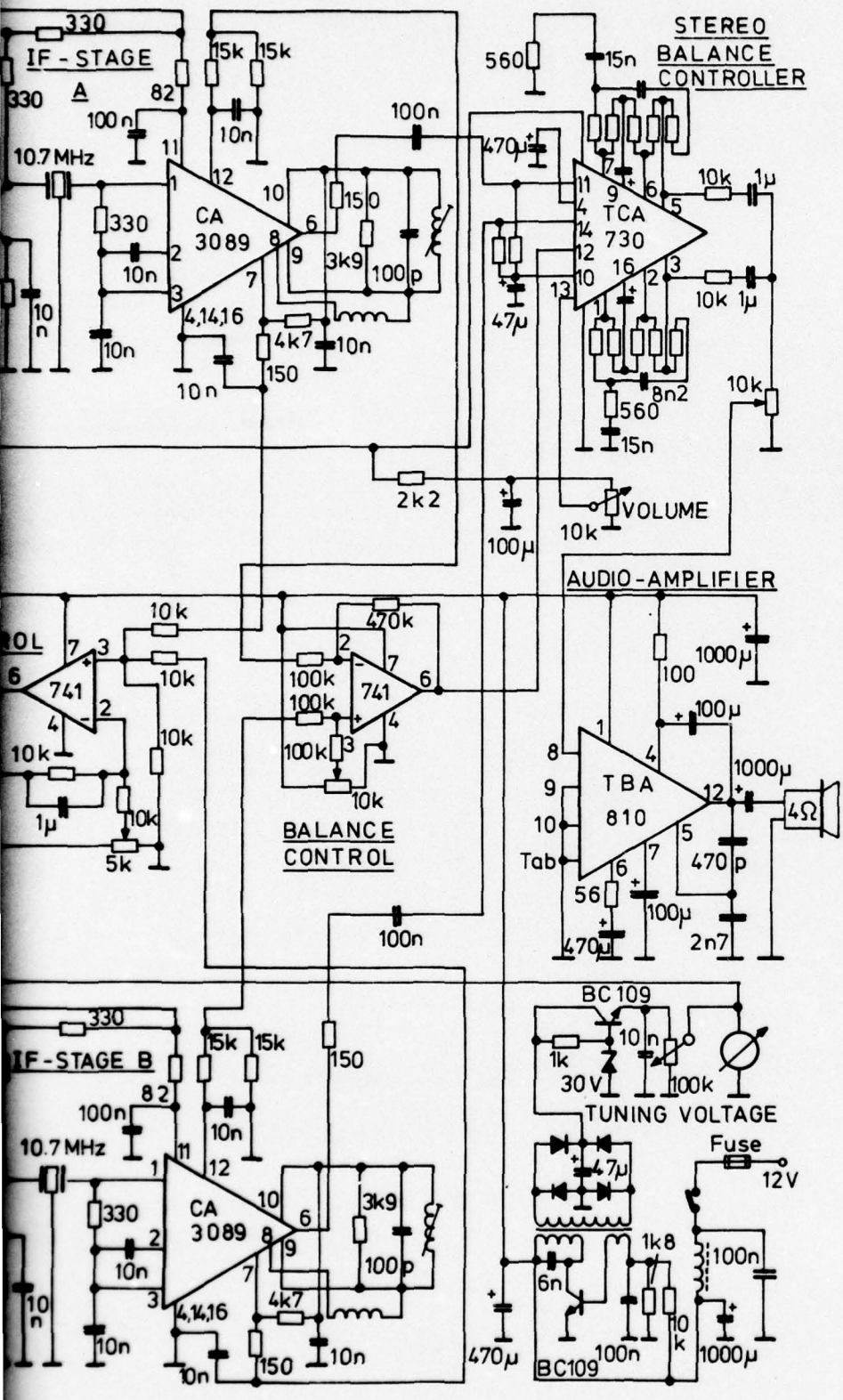

Fig. 29: Circuit diagram of the maximum ratio diversity receiver for the FM broadcast band.

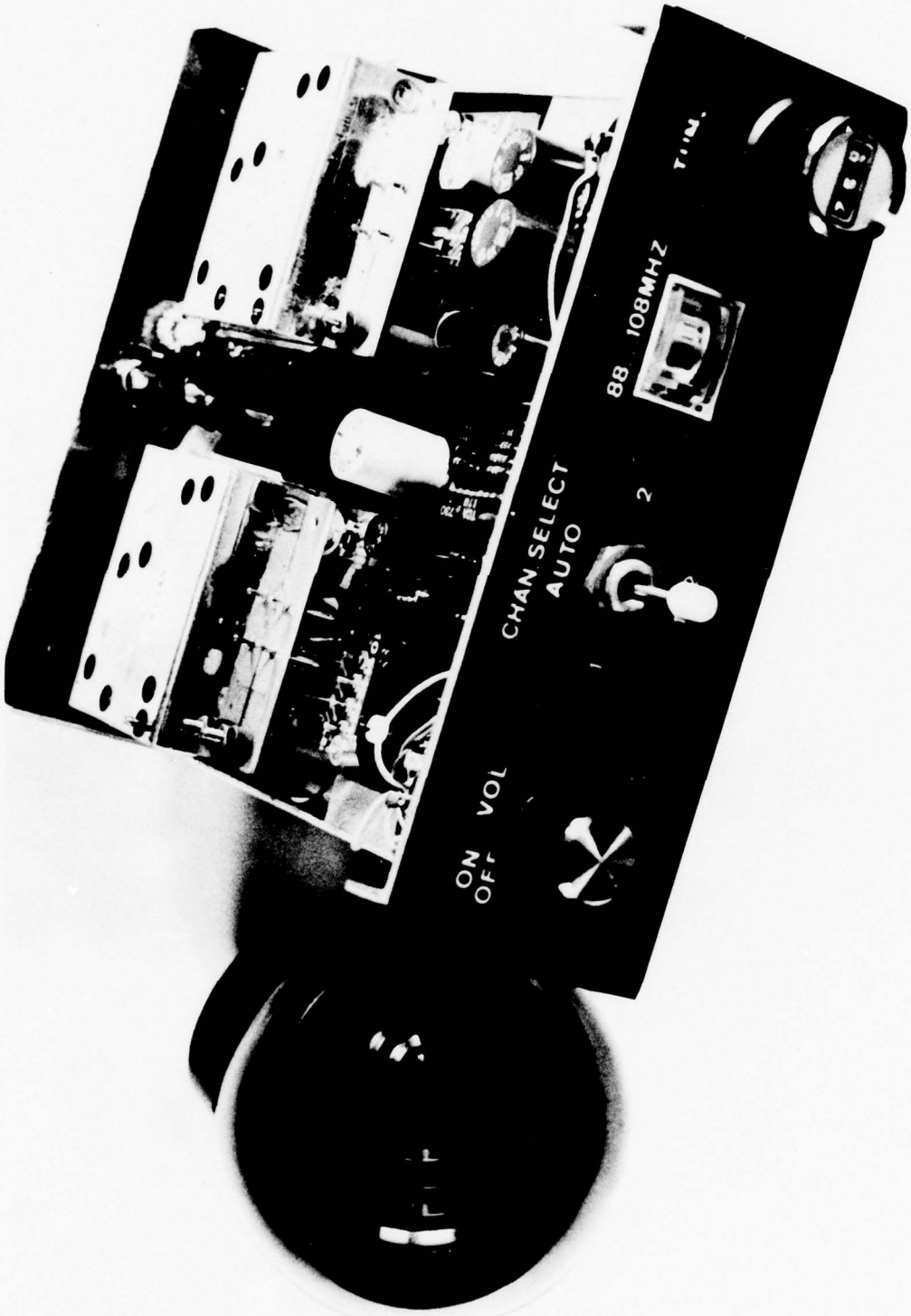

Fig. 30: Total view of the FM-test receiver

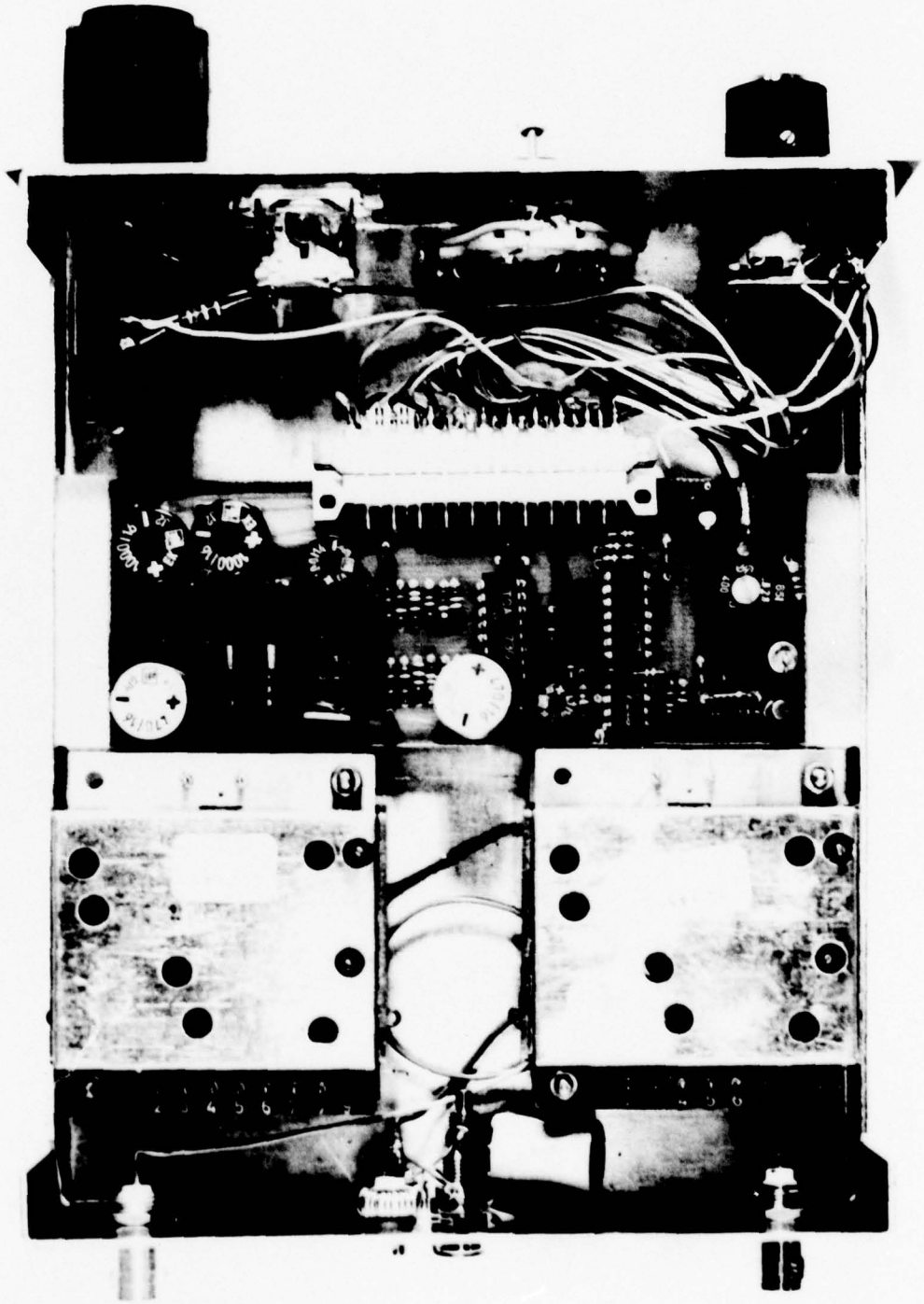

Fig. 31: Tuners, IF-amplifiers, control board and audio amplifier of the test receiver

7. Conclusion: Results and Recommendations

The measured covariance functions show that the correlation of two antennas mounted on a car is higher than the theory for a plane ground predicts for the same linear distance. On the other hand the correlation factors nevertheless are small enough to obtain sufficient diversity gain with the antenna distances realizable on cars.

The fade reduction is most effective in the case of equal RMS output voltages of the used antennas. A difference in the output voltages reduces the diversity gain. To find the optimum system one has to look for mounting places of the antennas where both conditions are fulfilled simultaneously: The normalized covariance function should not exceed a value of about 0.5 and the RMS values of the antennas broadbanded should be nearly the same.

Measurements of both conditions should be performed using a bearing car with the real military shape.

8.1 Literature cited

/1/ W.R. Young:
Comparison of Mobile Radio Transmission at 150, 450, 900, adn 3700 Mc
BSTJ, 1952, p.1068

/2/ J.F. Ossanna:
A Model for Mobile Radio Fading Due to Building Reflections: Theoretical and Experimental Fading Waveform Power Spectra, BSTJ, 1964, p. 2935

/3/ E.N. Gilbert:
Energy Reception for Mobile Radio
BSTJ, 1965, p. 1779

/4/ P.M. Trifonov, V.N. Budko, and V.S. Zotov:
Structure of USW Field Strength Spatial Fluctuations in a City, Trans. Telecommunications Radio Eng. 9, Pt. 1 (1964), pp. 26-30

/5/ H. Clarke:
A Statistical Theory of Mobile-Radio Reception
BSTJ, 1968, p. 957

/6/ H. Staras:
Diversity receiption with correlated signals,
J. Appl. Phys., Vol 27 (1956), pp. 93 - 94

/7/ S.O. Rice:
Mathematical analysis of random noise,
BSTJ, V. 24 (1945), pp. 46-156

/8/ A. Vigants:
Space Diversity Performance as a Function of Antenna Separation
IEEE Transaction on Com. Theory, Dec. 1968

/9/ M.J. Gans:
A Power Spectral Theory of Propagation in the Mobile-Radio Enviroment
IEEE Transactions on Vehicular Technology, February 1972

/10/ William C.-Y. Lee, Yu S. Yeh:
Polarization Diversity for Mobile Radio
IEEE Transactions on Communications, Oct. 1972

/11/ J.D. Parsons, P.A. Ratliff, M. Henze, M.J. Whiters:
Single-Receiver Diversity Systems,
IEEE Transactions on Vehicular Technology, November 1973

/12/ J.D. Parsons, Miguel Henze, P.A. Ratliff, Michael J. Whiters:
Diversity Techniques for Mobile Radio Reception,
IEEE Transactions on Vehicular Technology, August 1976

/13/ A.J. Rustako:
Evaluation of a Mobile Radio Multiple Channel Diversity Receiver using Pre-Detection Combining
IEEE Transactions on Vehicular Technology, October 1967

/14/ J.D. Parsons, P.A. Ratliff:
Self-phasing Aerial Array for FM-Communication Link
Electronics Letters, July 1971

/15/ T. Inatomi, H. Kohno, K. Ikai, B. Miyamoto:
IF Combined Space Diversity Reception
Fujitsu Scientific and Technical Journal, March 1972

/16/ P.A. Ratliff, J.D. Parsons, E.D.R. Shearman:
Space-Diversity Receiption for V.H.F. Mobile Radio
Electronics Letters, November 1971

/17/ M.J. Whiters:
Single Receiver Diversity for Reducing the Effect of Fast Fading in Mobile Radio
Electronics Letters, December 1971

/18/ A.J. Rustako, Y.S. Lee, R.R. Murray:
Performance of Feedback and Switch Space Diversity 900 MHz FM Mobile Radio Systems with Raleigh Fading
IEEE Transactions on Communications, November 1973

/19/ W.C.Y. Lee:
Effects on Correlation Between Two Mobile Radio Base-Station Antennas
IEEE Transactions on Communications, November 1973

/20/ D.M. Black, Douglas O. Reudink:
Some Characteristics of Mobile Radio Propagation at 836 MHz in the Philadelphia Area
IEEE Transactions on Vehicular Technology,
May 1972

/21/ D.C. Cox:
910 MHz Urban Mobile Radio Propagation:
Multipath Characteristics in New York City
IEEE Transactions on Communications,
November 1973

/22/ W.E. Shortall:
A Switched Diversity Receiving System for Mobile Radio
IEEE Transactions on Vehicular Technology,
November 1973

/23/ J.S. Bitler, H.H. Hoffmann, C.O. Stevens:
A Mobile Radio Single-Frequency "Two-Way" Diversity System Using Adaptive Retransmission from the Base
IEEE Transactions on Communications,
November 1973

/24/ B.R. Davis:
Random FM in Mobile Radio with Diversity
IEEE Transactions on Communications Theory,
December 1971

/25/ W.C. Jakes:
Microwave Mobile Communications,
John Wiley a. Sons, New York 1974

/26/ M. Schwartz, W.R. Bennett, S. Stein:
Communication Systems and Techniques,
McGraw Hill, New York, 1965, Chapters 10 and 11

/27/ D.G. Brennan:
Linear Diversity Combining Techniques,
Proc. IRE, 47 (1959), pp. 1075 - 1102

/28/ L. Tschimpke:
Statistische Untersuchungen beim Diversity-Empfang von Rayleigh-Feldern mit Kraftfahrzeugantennen, Doctor Thesis, University of the German Armed Forces Munich, to be finished in 1979

/29/ B. Kram:
Felstärke-Amplitudenverteilung bei einem mobilen Empfangssystem mit mehreren Antennen, Diploma Thesis, 1977, Univ. of the German Armed Forces Munich

/30/ W. Malchar:
Experimentelle Bestimmung von frequenzabhängigen Amplitudenverteilungen und Korrelationsfaktoren in einem mobilen Diversitysystem, to be finished in 1978, Univ. of the German Armed Forces Munich

/31/ W. Hader:
Mobile Empfangsanlage für gestörte Wellenfelder, Diploma Thesis, 1977, University of the German Armed Forces Munich

8.2 Selected Bibliography

/32/ S.W. Halpern:
The Theory of Operation of an Equal-Gain Predetection Regenerative Diversity Combiner with Rayleigh Fading Channels
IEEE Transactions on Communications Theory, August 1974

/33/ L. Lewin:
Diversity Reception and Automatic Phase Correction Proceedings of the IEE, July 1962

/34/ W.C.Y. Lee:
Statistical Analysis of the Level Crossings and Durations of Fades of the Signal from an Energy Density Mobile Radio Antenna
BSTJ, 1967, p. 417

/35/ H. Makino, K. Morita:
Design of Space Diversity Receiving and Transmitting Systems for Line-of-Sight Microwave Links IEEE Transactions on Communications Theory, 1967, p. 603

/36/ R.F. White:
Space Diversity on Line-of-Sight Microwave Systems
IEEE Transactions on Com Theory, 1968, p. 119

/37/ O.G. Villard, J.M. Lomasney, N.M. Kawachika:
A Mode-Averaging Diversity Combiner
IEEE Transaction on Com Theory, 1972, p. 463

/38/ T.A. Skinner, J.K. Cavers:
Selective Diversity for Rayleigh Rading Channels with a Feedback Link
IEEE Transactions on Com Theory, 1973, p. 117

/39/ S. Rhee, G. Zysman:
Results of Suburban Base Station Spatial Diversity Measurements in the UHF Band
IEEE Transactions on Com Theory, Oct. 1974

/40/ W.C.Y. Lee, R.H. Brandt:
The Elevation Angle of Mobile Radio Signal Arrival
IEEE Transactions on Communications, Nov. 1973

/41/ L. Schiff:
Statistical Suppression of Interference with Diversity in a Mobile-Radio Enviroment
IEEE Transactions on Vehicular Technology, Nov. 1972

/42/ D.O. Reudink:
Properties of Mobile Radio Propagation Above 400 MHz
IEEE Transactions on Vehicular Technology, Nov. 1974

/43/ D.O. Reudink, M.F. Wazowicz:
Some Propagation Experiments Relating Foliage Loss and Diffraction Loss at X-Band and UHF Frequencies.
IEEE Transactions on Vehicular Technology, Nov. 1973

/44/ W.C.Y. Lee:
Antenna Spacing Requirement for a Mobile
Radio Base-Station Diversity
BSTJ, 1971, p. 1859

9. List of Students and Graduate Students involved with the Research

Dipl.-Ing.	L. Tschimpke,	Doctor Thesis
Lt	B. Kram ,	Diploma Thesis
Lt	W. Malchar ,	Diploma Thesis
Lt	W. Hader ,	Diploma Thesis

Appendix:

BASIC-Program for the
Calculation of Correlation Factors

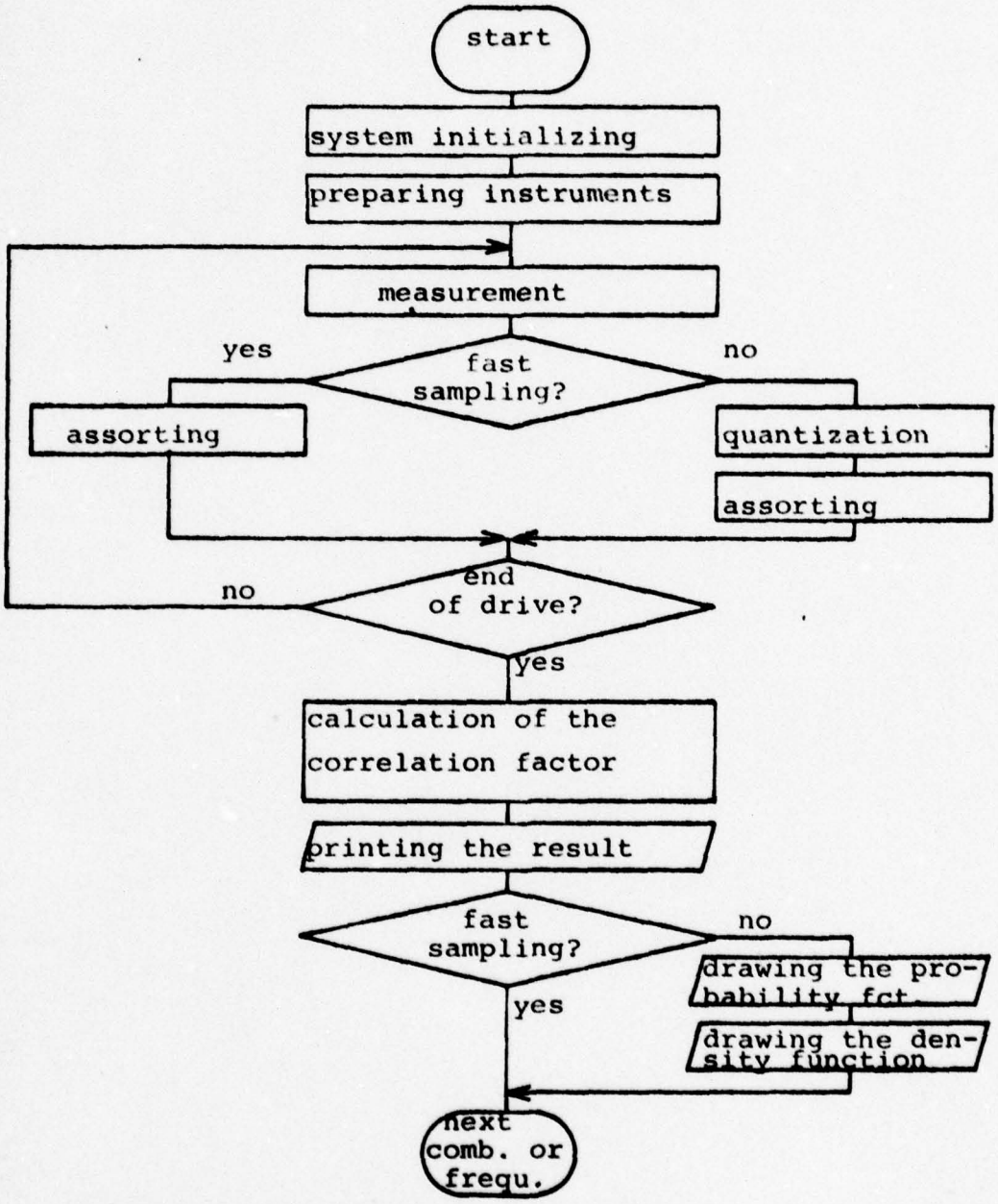

Fig. 32 Flow chart for the evaluation of the correlation factor

Appendix 1: Basic program for the evaluation or the correlation factor

```
4 GO TO 100
5 REM EINGABE
8 GO TO 166
9 GO TO 300
12 REM LANGSAMES ABTASTEN MIT QUANTISIEREN
13 Q2=1
14 PRINT "LANGSAME ABTASTUNG MIT QUANTISIEREN"
15 GO TO 170
16 REM SPEICHERN
17 GO TO 500
20 REM BERECHNEN
21 GO TO 700
24 REM ZEICHNEN
25 GO TO 2000
28 REM DICHTE ZEICHNEN
29 GO TO 2700
32 Y4=2
33 REM PLOTTER
34 GO TO 2020
36 REMAUFLISTEN DER SUMMEN-WK KEY 9
37 GO TO 3400
40 REM AUFLISTEN DER DICHTEN KEY 10
41 GO TO 3500
44 REM ERGEBNIS DRUCCKEN
45 GO TO 4000
48 REM HOLEN VOM BAND
49 GO TO 5000
56 REM HOLEN VOM BAND
57 GO TO 5000
100 INIT
101 SET KEY
102 N=40
103 M=37
105 DIM U(N),Z(3,N),Z4(N),H(3,N),P(3,N),C$(3),D$(4),E$(20)
110 Y1=31
115 P=0                                                ,F$(4),W(3,N)
120 A$="DRIVE No: "
130 B$=" ANTENNA COMBINATION: "
131 PRINT A$;" ? ";
132 INPUT C$
133 PRINT B$;" ? ";
134 INPUT D$
135 PRINT "FREQUENZ ? ";
136 INPUT F$
140 READ U
150 DAT -12,-11,-10,-9,-8,-7,-6,-5,-4,-3.5,-3,-2.5,-2,-1.5
160 DATA -0.25,0,0.25,0.5,0.75,1,1.5,2,2.5,3,3.5,4,5,6,7,8
165 DATA 13,14,15
```

```
166 Q2=0
167 PRINT "SCHNELLE ABTASTUNG"
170 ON SRQ THEN 1410
180 M$="F1R3A0H0M3T1D0"
190 PRINT @22:M$
200 PRINT @23:M$
210 U1=0
220 U2=0
230 U3=0
240 U4=0
250 U5=0
260 U6=0
265 P=0
266 D1=0
270 Y=0
280 REM
290 REM HOLEN VON DATEN
300 INPUT @22:A
310 INPUT @23:B
312 Y=Y+1
320 C=A*B
325 D=A+B
330 U1=U1+A*A
340 U2=U2+B*B
350 U3=U3+C
360 D1=D1+D
365 IF Q2=0 THEN 300
370 U4=U4+A
380 U5=U5+B
390 REM QUANT A
400 Q1=A
405 GOSUB 1500
410 P(1,I)=1+P(1,I)
415 REM QUANT B
420 Q1=B
425 GOSUB 1500
430 P(2,I)=1+P(2,I)
435 REM QUANT D
440 Q1=D
445 GOSUB 1500
450 REM
457 P(3,I)=1+P(3,I)
460 GO TO 300
470 REM QUANTISIERT
480 REM
481 REM
482 REM
500 PRINT "SPEICHERN AUF BAND ? 0=NEIN,SONST FILE-NR.: ";
510 INPUT Y2
520 IF Y2=0 THEN 620
530 FIND Y2
```

```
540 PRINT @33;C$
550 PRINT @33;D$
560 PRINT @33;F$
570 PRINT @33;M,Y,Q2,U1,U2,U3,U4,U5,D1
580 IF Q2=0 THEN 600
590 PRINT @33;P
600 PRINT @33;'ENDE'
605 CLOSE
610 PRINT 'DATEN SIND IN FILE ';Y2;' GESPEICHERT'
620 END
700 REM
704 V4=0
705 V5=0
710 REM BERECHNEN
711 V1=0
712 V2=0
713 V3=0
720 K=1
730 FOR J=1 TO 3
740 FOR I=1 TO M-1
750 P(J,I)=P(J,I)/Y
770 NEXT I
780 NEXT J
790 U1=U1/Y
800 U2=U2/Y
810 U3=U3/Y
820 U4=U4/Y
822 U5=U5/Y
824 D1=D1/Y
830 FOR J=1 TO 3
832 W(J,1)=1
834 FOR I=2 TO M-1
836 W(J,I)=W(J,I-1)-P(J,I-1)
840 NEXT I
842 W(J,M)=0
850 NEXT J
855 REM HOEHEN BERECHNEN
856 FOR I=1 TO M-1
861 U8=(U(I)+U(I+1))/2
862 REM GLAETTEN
863 IF ABS(U8)>0.5 THEN 872
864 U9=-U(I-1)-U(I)+U(I+1)+U(I+2)
865 FOR J=1 TO 3
866 H(J,I)=100*(P(J,I-1)+2*P(J,I)+P(J,I+1))/U9
867 NEXT J
868 GO TO 877
872 U9=U(I+1)-U(I)
873 FOR J=1 TO 3
875 H(J,I)=100*P(J,I)/U9
876 NEXT J
877 REM
```

```
890 V1=V1+U8^2*P(1,I)
900 V2=V2+U8^2*P(2,I)
905 V3=V3+U8*P(3,I)
910 V4=V4+U8*P(1,I)
920 V5=V5+U8*P(2,I)
930 NEXT I
935 IF Q2=0 THEN 950
940 R1=10*V3/SQR(V1*V2)
941 PRINT USING "14A,2D.4D":"AUS HIST. R1= ";R1
950 R=U3/SQR(U1*U2)
955 PRINT "  "
960 PRINT @32:" Aeff       Beff       A*B        Am         Bm"
970 PRINT @32: USING 971:SQR(U1),SQR(U2),U3,U4,U5
971 IMAGE3(3D.3D,4X),2D.5D,4X,2D.5D
980 PRINT @32:"KORREL.-FAKTOR R=";
981 PRINT @32: USING 982:R,A$,C$,B$,D$
982 IMAGE2D.4D,3X,4(FA)
984 PRINT USING "5A,2D.4D":"A+B= ";D1
990 END
1400 REM SERVICE ROUTINE
1410 POLL S1,S2;22;23;31;33
1415 POLL S3,S4;23
1420 RETURN
1500 REM SUBR.QUANTISIEREN
1510 Q=ABS(Q1)
1520 IF Q=>1 THEN 1550
1530 I=1+INT(4*Q)
1540 GO TO 1600
1550 IF Q=>4 THEN 1590
1560 I=3+INT(2*Q)
1570 GO TO 1600
1580 REM Q=>4
1590 I=7+INT(Q)
1600 IF I<18 THEN 1620
1610 I=18
1620 IF Q1<0 THEN 1650
1630 I=18+I
1640 GO TO 1670
1650 REM NEGATIVES Q1
1660 I=-I+19
1670 RETURN
1680 REM
1690 REM
2000 REM ZEICHNEN
2010 Y4=32
2020 PRINT "WELCHER SPANNUNGSBEREICH? MAX.10V ? ";
2021 INPUT K1
2022 K=10/K1
2030 PAGE
2040 U7=0
2050 VIEWPORT 10,70,55,90
2060 WINDOW -12,12,0,100
```

```
2070 H$="FARBE WECHSELN,DANN RETURN-KEY "
2080 FOR J=1 TO 3
2082 IF J<3 THEN 2090
2084 U7=U6
2090 MOVE @Y4:K*(U(1)-U7),W(J,1)*100
2100 FOR I=1 TO M
2110 DRAW @Y4:K*(U(I)-U7),W(J,I)*100
2120 GOSUB J OF 3200,3000,3100
2130 NEXT I
2140 IF Y4=32 THEN 2220
2150 PRINT H$,"GG"
2160 INPUT I$
2220 NEXT J
2221 GOSUB 2229
2222 GO TO 2600
2229 REM EINRAHMEN UND BESCHRIFTEN
2230 MOVE @Y4:-12,0
2240 DRAW @Y4:-12,100
2250 DRAW @Y4:12,100
2255 PRINT @Y4,17:1.1,1.8
2260 DRAW @Y4:12,0
2270 FOR I=0 TO 100 STEP 10
2280 MOVE @Y4:12,I
2290 DRAW @Y4:-12,I
2300 MOVE @Y4:-14.5,I-2
2310 PRINT @Y4: USING 2320:I
2320 IMAGE3D
2330 NEXT I
2340 MOVE @Y4:-14.5,105
2350 PRINT @Y4:" P/%"
2355 AXIS @Y4:1,5
2360 MOVE @Y4:-0.3,-7
2370 PRINT @Y4:"0"
2380 MOVE @Y4:-10.8,-7
2390 PRINT @Y4: USING 2391:-K1
2391 IMAGE3D.1D
2392 MOVE @Y4:-6.5,-7
2393 PRINT @Y4: USING 2391:-K1/2
2394 MOVE @Y4:8.5,-7
2395 PRINT @Y4: USING 2391:K1
2396 MOVE @Y4:3,-7
2397 PRINT @Y4: USING 2391:K1/2
2398 K2=4
2399 FOR S=-10 TO 10 STEP 5
2400 MOVE @Y4:S,-K2
2401 RDRAW @Y4:0,2*K2
2402 NEXT S
2410 GOSUB 4300
2420 RETURN
2700 REM ZEICHNEN DER DICHTEN
2701 U7=0
```

```
2705 WINDOW -12,12,0,100
2706 VIEWPORT 10,70,12,50
2707 MOVE @Y4:-11.8,105
2708 PRINT @Y4:"/V"
2710 FOR J=1 TO 3
2711 IF J<3 THEN 2720
2712 U7=U6
2720 MOVE @Y4:K*(U(1)-U7),0
2730 FOR I=1 TO M-1
2740 DRAW @Y4:K*(U(I)-U7),H(J,I)
2745 IF Y4=2 THEN 2752
2750 GOSUB J OF 3200,3000,3100
2752 DRAW @Y4:K*(U(I+1)-U7),H(J,I)
2753 IF Y4=2 THEN 2760
2755 GOSUB J OF 3200,3000,3100
2760 NEXT I
2770 DRAW @Y4:K*(U(M)-U7),0
2772 IF Y4=32 THEN 2780
2775 PRINT "GGGG",H$
2776 INPUT I$
2780 NEXT J
2810 GOSUB 2229
2812 WINDOW 0,100,0,100
2815 VIEWPORT 0,100,0,100
2820 MOVE @Y4:3,96
2825 PRINT @Y4,17:1.4,2.5
2830 PRINT @Y4:A$;C$;"  ";B$;D$;"    ";F$;" MHz"
2840 HOME
2850 PRINT @Y4,17:1,1.8
2860 MOVE @Y4:3,6
2870 PRINT @Y4:"RO=";
2880 PRINT @Y4: USING 982:R,A$,C$,B$,D$
2885 MOVE @Y4:3,3
2890 PRINT @Y4;"  Aeff        Beff        A*B        A+B"
2895 MOVE @Y4:3,0
2900 PRINT @Y4: USING "3(3D.3D,4X),2D.3D,1A":SQR(U1),SQR(U
2920 PRINT "GGGGGGGGG"
2930 END                                          2),U3,D1;"Ω";
3000 REM QUADRATE ZEICHNEN
3010 RMOVE @Y4:0.1,0.6
3020 RDRAW @Y4:-0.2,0
3030 RDRAW @Y4:0,-1.2
3040 RDRAW @Y4:0.2,0
3050 RDRAW @Y4:0,1.2
3060 RMOVE @Y4:-0.1,-0.6
3070 RETURN
3100 REM DREIECKE ZEICHNEN
3110 RMOVE @Y4:0,1
3120 RDRAW @Y4:-0.2,-1.5
3130 RDRAW @Y4:0.4,0
3140 RDRAW @Y4:-0.2,1.5
3150 RMOVE @Y4:0,-1
```

```
3160 RETURN
3200 REM KREUZE ZEICHNEN
3210 RDRAW @Y4:0.2,0
3220 RDRAW @Y4:-0.4,0
3230 RMOVE @Y4:0.2,0
3240 RDRAW @Y4:0,1
3250 RDRAW @Y4:0,-2
3260 RMOVE @Y4:0,1
3270 RETURN
3400 REM AUFLISTEN DER SUMMEM-WK  KEY 9
3405 PAGE
3410 T=32
3420 PRINT @T:"SUMMEN-WK ";A$;C$;"  ";B$;D$
3430 PRINT @T:"I    U(I)              W(1,I)          W(2,I)
3440 FOR I=1 TO M
3450 PRINT @T:I;"  ";U(I),W(1,I),W(2,I),W(3,I)     W(3,I)"
3460 NEXT I
3470 END
3500 REM AUFLISTEN DER WK-DICHTEN KEY10
3505 PAGE
3510 T=32
3520 PRINT @T:"WK-DICHTEN ";A$;C$;"  ";B$;D$
3530 PRINT @T:" I   U(I)           P(1,I)              P(2,I)
3540 FOR I=1 TO M-1
3550 PRINT @T:I;"  ";U(I),P(1,I),P(2,I),P(3,I)     P(3,I)"
3560 NEXT I
3570 END
4000 REM ERGEBNIS DRUCKEN
4005 PRINT @41: USING "2(""J""),100(""*"")":
4006 PRINT @41:A$;C$;"   ";B$;D$;"   ";F$;" MHz"
4007 PRINT @41: USING "100(""*"")":
4010 PRINT @41:"SAMPLES:";Y
4012 IF Q2=1 THEN 4016
4013 PRINT @41:"SAMPLING RATE:  65 Hz"
4015 GO TO 4020
4016 PRINT @41:"SAMPLING RATE:  25 Hz"
4020 PRINT @41:" Aeff      Beff      A*B       A+B"
4021 IMAGE8D,4X,3(2D.3D,4X),2D.5D,4X,2D.5D                'Y,D1/Y
4030 PRINT @41: USING "4(2D.3D,4X)":SQR(U1/Y),SQR(U2/Y),U3/
4045 PRINT @41: USING "4A,2D.4D":"RO= ";U3/SQR(U1*U2)
4050 PRINT "ENTER TEXT !G"
4060 INPUT L$
4070 PRINT @41:L$
4090 PRINT @41: USING "100(""*""),""J""":
4100 END
4300 REM PFEIL
4310 MOVE @Y4:11,-7
4320 RDRAW @Y4:1,0
4330 RDRAW @Y4:-0.2,0.2
4340 RMOVE @Y4:0,-0.4
4350 RDRAW @Y4:0.2,0.2
```

```
4360 RMOVE @Y4:0.3,-0.3
4370 PRINT @Y4:'G*/H_H\Ain volts'
4380 RETURN
5000 REM DATEN HOLEN VOM BAND
5010 PRINT 'WELCHES FILE LESEN? '
5020 INPUT Y2
5030 IF Y2=0 THEN 5200
5040 FIND Y2
5050 INPUT @Y2:C$
5060 INPUT @Y2:D$
5070 INPUT @Y2:F$
5080 INPUT @Y2:M,Y,Q2,U1,U2,U3,U4,U5,D1
5090 IF Q2=0 THEN 5110
5100 INPUT @33:P
5110 INPUT @33:E$
5120 IF E$='ENDE' THEN 5130
5130 GO TO 5150
5140 PRINT 'FEHLER BEI DATENUEBERNAHME!GGGG'
5150 PRINT A$;C$,B$;D$,'FREQUENZ ';F$
5160 PRINT 'M=';M,'Y=';Y,'Q2=';Q2
5170 PRINT 'U1=';U1,'U2=';U2,'U3=';U3
5180 PRINT 'DATEN AUS FILE-NR. ';Y2
5190 END
5200 END
```

Appendix:

BASIC-Program for the
Calculation of the Fade Reduction

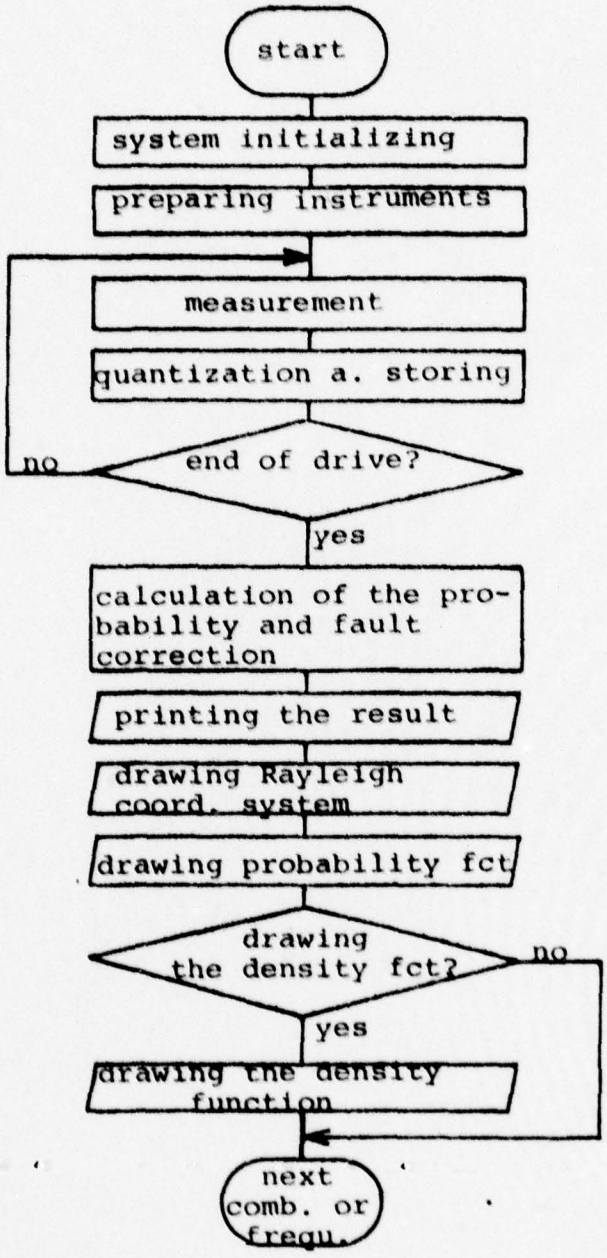

Fig. 33: Flow chart for the evaluation of the probability that the received signals exceed a certain threshold

Appendix 2:

Basic program for the evaluation of the probability that the received signals exceed a certain threshold

```
4 GO TO 100
8 REM NEUE DATEN
9 GO TO 330
20 REM BERECHNEN
21 GO TO 600
24 REM ZEICHNEN
25 GO TO 1120
32 REM PLOTTER ZEICHNEN
33 Z=2
34 GO TO 1140
36 REM EINZEICHNEN DER SUMMEN-WK
37 GO TO 1900
44 REM AUSDRUCKEN DER SUMMEN-WK DER EINZELKANAELE
45 GO TO 2710
98 REM
99 REM
100 INIT
110 SET KEY
120 N=230
130 DIM P(4,N),J1(4),M(4),P1(30),M8(4),U9(4)
140 FOR K=1 TO 22
150 READ P1(K)
160 DATA 0.01,0.1,1,5,10,20,30,40,50,60,70,80,90
170 DATA 95,98,99,99.6,99.8,99.9,99.96,99.98,99.99
180 NEXT K
190 U9=0
200 L4=0
210 A$="DRIVE NO.:"
220 B$="ANTENNA COMB.:"
230 ON SRQ THEN 1000
240 M$="F1R3A0H0M3T1D0"
250 PRINT @22:M$
260 PRINT @23:M$
270 PRINT A$;"? ";
280 INPUT C$
290 PRINT B$;"? "
300 INPUT D$
310 PRINT "FREQUENCY? "
320 INPUT F$
330 Y=0
340 P=0
350 REM ENDE DER VORBEREITUNG
360 REM
```

```
370 REM
400 REM HOLEN VON DATEN
410 INPUT @22:A
420 INPUT @23:B
430 A=ABS(A)
440 B=ABS(B)
450 Y=1+Y
460 K=1+(A<=1)*100*A+(A>1)*(90+10*A)
470 P(1,K)=1+P(1,K)
480 L=1+(B<=1)*100*B+(B>1)*(90+10*B)
490 P(2,L)=1+P(2,L)
500 M1=K MAX L
510 P(3,M1)=1+P(3,M1)
520 C=0.5*(A+B)
530 M2=1+(C<=1)*100*C+(C>1)*(90+10*C)
540 P(4,M2)=1+P(4,M2)
550 GO TO 410
560 REM ENDE DER EINGABE
570 REM
580 REM
590 REM
600 REM BERECHNEN DER SUMMENWK(UNTERSCHREITUNG)
610 FOR I=1 TO 4
620 P(I,1)=P(I,1)/Y
630 FOR J=2 TO N
640 P(I,J)=P(I,J-1)+P(I,J)/Y
650 IF NOT(P(I,J)=>0.5 AND P(I,J-1)<0.5) THEN 670
660 J1(I)=J
670 NEXT J
680 NEXT I
690 REM BERECHNEN DER 50%-WERTE DURCH INTERPOLATION
700 FOR I=1 TO 4
710 J=J1(I)-1
720 GOSUB 900
730 U1=U
740 J=J1(I)
750 GOSUB 900
760 U2=U
770 M(I)=U1+(U2-U1)*(0.5-P(I,J-1))/(P(I,J)-P(I,J-1))
780 M(I)=20*LGT(M(I))+6*(I=4)
790 NEXT I
800 PRINT " M1/dB      M2/dB      M3/dB      M4/dB GGGGGGG"
810 PRINT USING "4 (2D.3D,4X)":M(1),M(2),M(3),M(4)
820 M8=M
830 L4=M(1) MAX M(2)
840 END
850 REM
860 REM
```

```
900 REM SUBROUTINE:BERECHNEN VON U AUS DEM DIG. PUNKT J
910 IF J>100 THEN 940
920 U=J/100
930 RETURN
940 U=J/10-9
950 U=U+(U>5)*(U-5)*0.087
960 RETURN
990 REM
1000 REM SERVICE ROUTINE
1010 POLL S1,S2;22;23;31;33
1020 POLL S1,S2;23
1030 RETURN
1040 REM
1050 REM
1100 REM DRUCKEN VON WAHRSCHEINLICHKEITSPAPIER FUER EINE
1110 REM RAYLEIGHVERTEILUNG
1120 Z=32
1130 PAGE
1140 V1=7.8
1150 V2=65.8
1160 V3=20
1170 V4=95
1180 V5=12.4
1190 V6=42
1200 WINDOW -45,24.9,-20,50
1210 VIEWPORT V1,V2,V3,V4
1220 PRINT @Z,17:0.6,1.3
1230 A1=-11.2345
1235 REM VERTIKALE LINIEN
1240 FOR L=-40 TO 20 STEP 5
1250 MOVE @Z:L,A1
1260 DRAW @Z:L,40
1270 MOVE @Z:L-1,A1-2
1280 PRINT @Z: USING 1290:L
1290 IMAGE +2D
1300 NEXT L
1310 MOVE @Z:18,-15
1320 PRINT @Z:"level/dB"
1330 REM HORIZONTALE LINIEN
1340 FOR K=1 TO 22
1350 Y1=LOG(100/P1(K))/LOG(2)
1360 Y1=-10*LGT(Y1)
1370 MOVE @Z:-40.5,Y1
1380 DRAW @Z:20,Y1
1390 MOVE @Z:-44.9,Y1-0.5
1400 PRINT @Z: USING 1430:P1(K)
1410 MOVE @Z:20.8,Y1-0.5
1420 PRINT @Z: USING 1430:100-P1(K)
1430 IMAGE 2D.2D
1440 NEXT K
```

```
1450 MOVE @Z:-44,41.5
1460 PRINT @Z:"P /%"
1470 MOVE @Z:22,41.5
1480 PRINT @Z:"P /%"
1490 RESTORE
1500 REM
1510 MOVE @Z:-35,44
1520 PRINT @Z,17:1,2
1530 PRINT @Z:A$;C$;"   ";B$;D$;"   ";"f=";F$;" MHz"
1540 GO TO 1900
1550 PRINT @Z,17:0.6,1.3
1560 REM
1570 REM
1580 REM DICHTE ZEICHNEN
1590 WINDOW -45,24.9,-1.3,10
1600 VIEWPORT V1,V2,V5,V6
1610 FOR L=-40 TO 20 STEP-5
1620 MOVE @Z:L,0
1630 DRAW @Z:L,10
1640 MOVE @Z:L-1,-0.6
1650 PRINT @Z: USING 1290:L
1660 NEXT L
1670 MOVE @Z:15,-1
1680 MOVE @Z:18,-1.3
1690 PRINT @Z:"level/dBK"
1700 REM HORIZONTALE LINIEN
1710 FOR I=0 TO 10 STEP 2
1720 MOVE @Z:-40.5,I
1730 DRAW @Z:20.5,I
1740 MOVE @Z:-44,I-0.2
1750 PRINT @Z: USING "2D":2*I
1760 NEXT I
1770 MOVE @Z:-44,10.5
1780 PRINT @Z:" P/ %/dB"
1790 PRINT "GGGGGG"
1800 REM FORMBLATT FERTIG
1810 REM
1820 REM
1830 REM
1900 REM EINZEICHNEN DER SUMMEN-WK
1910 WINDOW -45,24.9,-20,50
1920 VIEWPORT V1,V2,V3,V4
1930 U1=1
1940 L3=0
1950 L2=LOG(2)
1960 FOR I=1 TO 4
1970 K1=1
1980 FOR J=1 TO N STEP K1
1990 GOSUB 900
2000 X1=(U-U9(I))*(U>U9(I))+(U<=U9(I))*0.01
2010 L=20*LGT(X1)-L3+6*(I=4)-L4
2020 Q=1-P(I,J)
```

```
2030 IF Q<0.9999 THEN 2050
2040 Q=0.9999
2050 IF Q>1.0E-4 THEN 2070
2060 Q=1.0E-4
2070 Y1=-LOG(Q)/L2
2080 IF L>20.2 THEN 2160
2090 H=-10*LGT(Y1)
2100 IF J>1 THEN 2120
2110 MOVE @Z:L,H
2120 DRAW @Z:L,H
2130 IF J<20 THEN 2150
2140 K1=2
2150 NEXT J
2160 NEXT I
2170 PRINT 'GGG'
2180 GO TO 2490
2190 REM EINZEICHNEN DER SUMMENHAEUFIGKEIT BEENDET
2200 REM
2210 REM EINZEICHNEN DER DICHTE
2220 WINDOW -45,24.9,-1.3,10
2230 VIEWPORT V1,V2,V5,V6
2240 FOR I=1 TO 4
2250 MOVE @Z:-40,0
2260 U1=0.01
2270 J2=1
2280 J=1
2290 REM
2300 J=J+1
2310 GOSUB 900
2320 U2=U
2330 L2=20*LGT(U2/U1)
2340 IF J=N THEN 2360
2350 IF L2<1.5 THEN 2300
2360 REM PASSENDES INTERVALL GEFUNDEN, ZEICHNEN
2370 H=50*(P(I,J)-P(I,J2))/L2
2380 X1=(U1-U9(I))*(U1>U9(I))+(U1<=U9(I))*0.01
2390 L1=20*LGT(X1)-L3+6*(I=4)-L4
2400 DRAW @Z:L1,H
2410 DRAW @Z:L1+L2,H
2420 U1=U2
2430 J2=J
2440 IF J<N THEN 2290
2450 DRAW @Z:L1+L2,0
2460 NEXT I
2470 REM EINZEICHNEN DER DICHTE BEENDET
2480 REM
2490 VIEWPORT 20,75,15,40
2500 PRINT @Z,17:0.9,1.6
2510 MOVE @Z:-40,-1
2520 M8=M-L3-L4
2530 PRINT @Z:' Am        Bm      (AmaxB)m    (A+B)m'
```

```
2540 MOVE @Z:-43,-9
2550 PRINT @Z: USING "4(+2D.1D,    ""dB"",3X), ""K""":M8
2560 HOME
2570 PRINT "ENTER COMMENTAR! "
2580 INPUT E$
2590 MOVE @Z:-43,-17
2600 PRINT @Z:E$,"KK"
2610 PRINT "GGGGGGG"
2620 END
2630 REM KOMPLETTE ZEICHNUNG FERTIG
2640 REM
2650 REM
2660 REM
2700 REM AUSDRUCKEN DER INTERVALLE,SPG,PEGEL,EINZEL-WK
2710 PRINT @41:
2720 PRINT @41:"  J         U         dB        Pa         Pb
2730 PRINT @41:
2740 FOR J=1 TO N STEP 4
2750 GOSUB 900
2760 PRINT @41: USING 2780:J,U,20*LGT(U)-L3,1-P(1,J),1-P(
2770 NEXT J
2780 IMAGE 3D,4X,-2D.3D,4X,-2D.1D,4X,2(1D.4D,4X)
2790 END
2800 REM
```